

Modeling of Riverbed incision and evolution of Transient landscape

Dr. N.L. Dongre



The Denwa River of Pachmarhi. Transiency is not limited to individual rivers but also affects larger systems such as the Pachmarhi of India where the landscape may never reach a condition of steady state due to the permanent asymmetry in vertical uplift, climatically driven denudation and horizontal tectonic advection.

Abstract. Landscape evolution models allow studying the earth surface response to a changing climatic and tectonic forcing. While much effort has been devoted to the development of Landscape evolution models that simulate a wide range of processes, the numerical accuracy of these models has received much less attention. Most Landscape evolution models use first order accurate numerical methods that suffer from substantial numerical diffusion. Numerical diffusion particularly affects the solution of the advection equation and thus the simulation of retreating landforms such as cliffs and river knick points with potential unquantified consequences for the integrated response of the simulated landscape. Here we present topotoolbox landscape evolution models, a spatially explicit, raster based landscape evolution model for the study of fluvial eroding landscapes in TopoToolbox 2. Topotoolbox landscape evolution models prevents numerical diffusion by implementing modulating a higher order flux limiting total volume method that is total variation diminishing (total variation diminishing -finite volume method) and solves the partial differential equations of river incision and tectonic displacement. We show that the choice of the total variation diminishing -finite volume method to simulate river incision significantly influences the evolution of simulated landscapes and the spatial and temporal variability of catchment wide erosion rates. Furthermore, a 2D total variation diminishing -finite volume method accurately simulates the evolution of landscapes affected by lateral tectonic displacement, a process whose simulation is hitherto largely limited to Landscape evolution models with flexible spatial discretization. By providing accurate numerical schemes on rectangular grids, topotoolbox landscape evolution models is a widely accessible landscape evolution model that is compatible with GIS analysis functions from the TopoToolbox interface.

1. Introduction

[1] Landscape evolution models simulate how the earth surface evolves in response to different driving forces including tectonics, climatic variability and human activity. Landscape evolution models are integrative as they amalgamate empirical data and conceptual models into a set of mathematical equations that can be used to reconstruct or predict terrestrial landscape evolution and corresponding sediment fluxes (Howard, 1994). Studies that address how climate variability and land use changes will affect landscapes on the long term increasingly rely on Landscape evolution models (Gasparini and Whipple, 2014).

[1.2] A large number of geophysical processes act on the earth surface, mostly driven by gravity and modulated by the presence of water, ice and organisms (Braun and Willett, 2013). These processes critically depend on the availability potential energy, brought into or withdrawn from the landscape by tectonic forces (Wang et al., 2014). Weathering and erosion respond to tectonic uplift, shaping the landscape through the lateral transport of sediments and, to a certain degree, also through feedback on regional uplift patterns (Whipple and Meade, 2004).

[1.3] Landscape evolution models allow integrating growing field evidence covering different spatial and temporal timescales (Glotzbach, 2015), thereby accommodating a broad range of applications with fundamental importance in the development of geosciences (Bishop, 2007). Landscape evolution models are key to understanding landscape evolution both over time scales of millions of years (van der Beek and Braun, 1998; Tucker and Slingerland, 1994; Willett et al., 2014; Willgoose et al., 1991b) and much shorter, millennial, timescales (Coulthard et al., 2012). Landscape evolution models simulate the interaction between different processes and provide insights into how these interactions result in different landforms. Moreover, visualizing landscape

evolution model output in intuitive animations stimulates the development of new theories and hypotheses (Tucker and Hancock, 2010). Landscape evolution models have also successfully been used for higher education in geomorphology and geology, improving students understanding of geophysical processes (Luo et al., 2016).

[1.4] Landscape evolution is not always smooth and gradual. Instead, sudden tectonic displacements along tectonic faults can create distinct landforms with sharp geometries (Whittaker et al., 2007). These topographic discontinuities are not necessarily smoothed out over time, but may persist over long time scales in transient landscapes (Mudd, 2016). For example, faults may spawn knickpoints along river profiles. These knickpoints will propagate upstream as rapids or water falls (Hoke et al., 2007), thereby maintaining their geometry through time (Campforts and Govers, 2015). After an uplift pulse, the river will only regain a steady state when the knickpoint finally arrives in the uppermost river reaches. Transiency is not limited to individual rivers but also affects larger systems such as the Pachmarhi of India where the landscape may never reach a condition of steady state due to the permanent asymmetry in vertical uplift, climatically driven denudation and horizontal tectonic advection

[1.5] Topographic discontinuities that result from transient 'shocks' are inherently difficult to model accurately. Most of the widely applied Landscape evolution models (Valters, 2016), use first order accurate explicit or implicit finite difference methods to solve the partial differential equations (partial differential equation) that are used to simulate river incision. These schemes suffer from numerical diffusion (Campforts and Govers, 2015; Royden and Perron, 2013). Numerical diffusion will inevitably lead to the gradual disappearance of knickpoints: the inherent inaccuracy of (implicit) first order accurate methods will result in ever smoother shapes. While this topographic smearing has already been shown to have implications for the accuracy of modelled longitudinal river profiles, we hypothesize that it is also relevant for the simulation of hillslope processes: hillslopes respond to river incision and, thus, inaccuracies in river incision modelling will propagate to the hillslope domain. Whether and to what extent this occurs, is yet unexplored.

[1.6] Tectonic displacement is similar to river knick point propagation; in both cases, sharp landscape forms are laterally moving. Numerical diffusion may therefore significantly alter landscape features when tectonic shortening or extension is simulated using first order accurate methods. This problem Landscape evolution model can in principle be overcome with flexible gridding, whereby the density of nodes on the modelling domain is dynamically adapted to the local rate of change in topography. However, models using flexible gridding have other constraints. They are much more complex to implement Landscape evolution model and hence less easy to adapt, require permanent mesh grid updates and impose the structure of the numerical grid to the natural drainage network as rivers are forced to follow the numerically composed grid structure. Furthermore, the output of flexible grid models is not directly compatible for most software that is available for topographic analysis (Schwanghart and Kuhn, 2010).

[1.7] Here we present topotoolbox landscape evolution models, a spatially explicit raster based landscape evolution model, which is based on the object-oriented (Benjamin Campforts, Wolfgang Schwanghart and Gerard Govers-2016) function library topotoolbox 2 (Schwanghart and Scherler, 2014). Contrary to previously published Landscape evolution models we solve river incision using a flux limiting total volume method which is total variation diminishing (total variation diminishing) in order to prevent numerical diffusion when solving the stream power law. Our numerical scheme expands on previous work (Campforts and Govers, 2015) by extending the mathematical formulation of the total variation diminishing method from 1D to entire river networks. Moreover, we developed a 2D total variation diminishing-finite volume

method to simulate horizontal tectonic displacement on regularly grids, thus allowing accounting for three dimensional variations in tectonic deformation. The objective of this paper is to evaluate topotoolbox landscape evolution models and assess the performance of the numerical methods to a variety of real-world and synthetic situations. We show that the use of this updated numerical method has implications for the simulation of both catchment wide erosion rates and landscape topography over geological time scales.

[1.8] Topotoolbox landscape evolution models provide the geoscientific community with an easily accessible and adaptable tool. Topotoolbox landscape evolution models are therefore a fully open source software package, written in MATLAB and based on the TopoToolbox platform. Users should be able to run topotoolbox landscape evolution models using both real data and synthetic landscapes. Moreover, the integration of topotoolbox landscape evolution models in TopoToolbox allows direct digital 80 terrain analysis using the TopoToolbox library (Schwanghart and Scherler, 2014). In its current form topotoolbox landscape evolution models is limited to uplifting, fluvially eroding landscapes: further development will allow integrating other processes (e.g. glacial erosion) as well as the explicit routing of sediment through the landscape.

2. Theory and geomorphic transport laws

2.1. Tectonic deformation

In its simplest form, tectonic deformation is represented by vertical uplift; $U(x, y, t)$ [$L t^{-1}$]. however, many tectonic configurations imply that displacements have both a vertical (uplift or subsidence) and a lateral (extension or shortening) component (Willett, 1999; Willett et al., 2001). The change in elevation of the earth surface (z) over time due to tectonic deformation is then:

$$\frac{\partial z}{\partial t} = U + v_x \frac{\partial z}{\partial x} + v_y \frac{\partial z}{\partial y} \quad (1)$$

where V_x and V_y [$L t^{-1}$]. are the tectonic displacement velocities in the x and y direction, respectively.

2.2. River incision

Detachment limited fluvial erosion is calculated based on the well-established relation between the channel gradient and the contributing drainage area (A), also referred to as the Stream Power Law (Howard and Kerby, 1983):

$$\frac{\partial z}{\partial t} = -K_{wk} (w_A A)^m \left(\frac{\partial z}{\partial x} \right)^n \quad (2)$$

K [$L^{1-2m} t^{-1}$] is an erodibility parameter that depends on local climate, hydraulic roughness, lithology and sediment load. K can be adapted to local variations in erodibility by using a scaling coefficient w_K [dimensionless]. In case of uniform erodibility, w_K is set to one. A is the drainage area, which is used as a proxy for the local discharge. Similar to K , A can be corrected for regional precipitation variabilities through a scaling coefficient w_A [dimensionless]. m and n represent the area and slope exponent: their values reflect hydrological conditions, channel width, as well as the dominant erosion mechanism. K , m and n are interdependent and it is usually impractical to constrain any of their values alone (Croissant and Braun, 2014; Lague, 2014). Thus, many studies provide estimates for the m/n ratio. For m/n ratios between 0.35 and 0.8, K

values span several orders of 100 magnitudes between $10^{-10} - 10^{-3} \text{ m}^{(1-2\text{m})} \text{ yr}^{-1}$ (Kirby and Whipple, 2001; Seidl and Dietrich, 1992; Stock and Montgomery, 1999). In order to represent fluvial sediment transport, it has previously been proposed to add a diffusion component (Rosenbloom and Anderson, 1994). However, we follow others in assuming that in eroding settings, detachment limited erosion is controlling landscape evolution and is represented by the advection equation represented in Eq. (2) (Attal et al., 2008; Goren et al., 2014; Howard and Kerby, 1983; Whipple and Tucker, 1999).

2.3. Hillslope processes

River incision drives the development of erosional landscapes by changing the base level for hillslope processes. Steepening of hillslopes subsequently leads to increased sediment fluxes from hillslopes to the river system. Hillslope erosion is equal to the divergence of the flux of soil/regolith material ($\mathbf{q}_s, [L^3 L^{-1} T^{-1}]$):

$$\frac{\partial z}{\partial t} = -\nabla \cdot \mathbf{q}_s \quad (3)$$

Different geomorphological laws describe hillslope response to lowering base levels. The model of linear diffusion assumes that the soil/regolith flux is proportional to the hillslope gradient (Culling, 1963):

$$\mathbf{q}_s = -D \nabla_z \quad (4)$$

where D is the diffusivity [$L^2 t^{-1}$] that parameterizes hillslope erosivity and erodibility and determines rate of soil/regolith creep. Linear hillslope diffusion produces convex upward slopes. Field evidence, however, suggests that this model is only rarely appropriate (Dietrich et al., 2003). Instead, hillslopes often tend to have convex-planar profiles because rapid, ballistic particle transport and shallow landsliding dominate as soon as slopes approach or exceed a critical angle (DiBiase et al., 2010; Larsen and Montgomery, 2012). To account for this rapid increase of flux rates with increasing slopes, Andrews and Bucknam (1987) and Roering et al. (1999) proposed a nonlinear formulation of diffusive hillslope transport, assuming that flux rates increase to infinity if slope values approach a critical slope S_c :

$$\mathbf{q}_s = -\frac{D \nabla_z}{1 - (|\nabla_z|/S_c)^2} \quad (5)$$

Main controls on variations of D include substrate, lithology, soil depth, climate and biological activity, amongst others. Values of D vary widely and range between 10^{-3} and $10^{-1} \text{ m}^2 \text{ yr}^{-1}$ for slopes under natural land use (Campforts et al., 2016; DiBiase and Whipple, 2011; Jungers et al., 2009; Roering et al., 1999; West et al., 2013).

2.4. Overall landscape evolution

In summary, topotoolbox landscape evolution models solve the following partial differential equations: First, it simulates the horizontal tectonic displacements over the entire model domain:

$$\frac{\partial z}{\partial t} = v_x \frac{\partial z}{\partial x} + v_y \frac{\partial z}{\partial y} \quad (6)$$

Second, top toolbox landscape evolution models simulate detachment limited river incision for the parts of the landscape that are predominantly sculpted by fluvial processes. We determine that domain where contributing drainage area (4) exceeds a critical drainage area (A_c):

$$\frac{\partial z}{\partial t} = U + \left(v_x \frac{\partial z}{\partial x} + v_y \frac{\partial z}{\partial y} \right) - \left(K w_k (w_A A)^{(m+var(m))} \left(\frac{\partial z}{\partial x} \right)^n \right) \quad (7)$$

Where $var(m)$ refers to the variability on m which is explained further (Eq. (20)).

Third, we define the hillslope domain where $A < A_c$. Topographic changes in this domain are calculated by:

$$\frac{\partial z}{\partial t} = \frac{\rho_r}{\rho_s} U - \nabla q_s \quad (8)$$

Where ρ_r and ρ_s are the bulk densities of the bedrock and the regolith material, respectively [$m L^3$]. The formulation of Eq. (8) implies that we assume that hillslopes are generally covered by regolith and/or soil.

3. Implement Landscape evolution modelation and numerical schemes of topotoolbox landscape evolution models`

Our main motivation to develop topotoolbox landscape evolution models is to provide users with a multi-process landscape evolution model that has a good overall computational performance and high numerical accuracy. Topotoolbox landscape evolution models is predominantly written in the MATLAB programming language; to reduce run times, however, topotoolbox landscape evolution models encompasses some C-code where this significantly improves 140 performances. Integrating topotoolbox landscape evolution models into TopoToolbox enables running the model, visualizing and analyzing its output in the same computational environment.

Figure 1 shows a schematic representation of the topotoolbox landscape evolution models workflow. Users can configure the tectonic setting by providing (i) a 2D or 3D array that represents spatially and spatio-temporally variable vertical uplift patterns, respectively, and (ii) two matrices to represent horizontal velocity fields (v_x and v_y). Topotoolbox landscape evolution models accepts synthetic topographies and real world digital elevation models and 145 leaves users with full control on model parameter values. In the following sections, we will discuss the numerical methods involved in top toolbox landscape evolution models to solve the partial differential equations described in section 2. The section numbers correspond to the processes indicated in the workflow in Fig. 1.

3.1. Drainage network development

TopoToolbox provides a function library for deriving and updating the drainage network and terrain attributes in MATLAB 150 (Schwanghart and Scherler, 2014). The calculation of flow-related terrain attributes, i.e., data derived from flow directions, relies on a set of highly efficient algorithms that exploit the directed and acyclic graph structure of the river flow network (Phillips et al., 2015). Nodes of the network represent grid cells and edges represent the directed flow connections between the cells in downstream direction. Topological sorting of this network of grid cells transforms returns an ordered list of cells in that upstream cells appear before their downstream neighbors. Based on this list, we calculate terrain attributes such as upslope 155

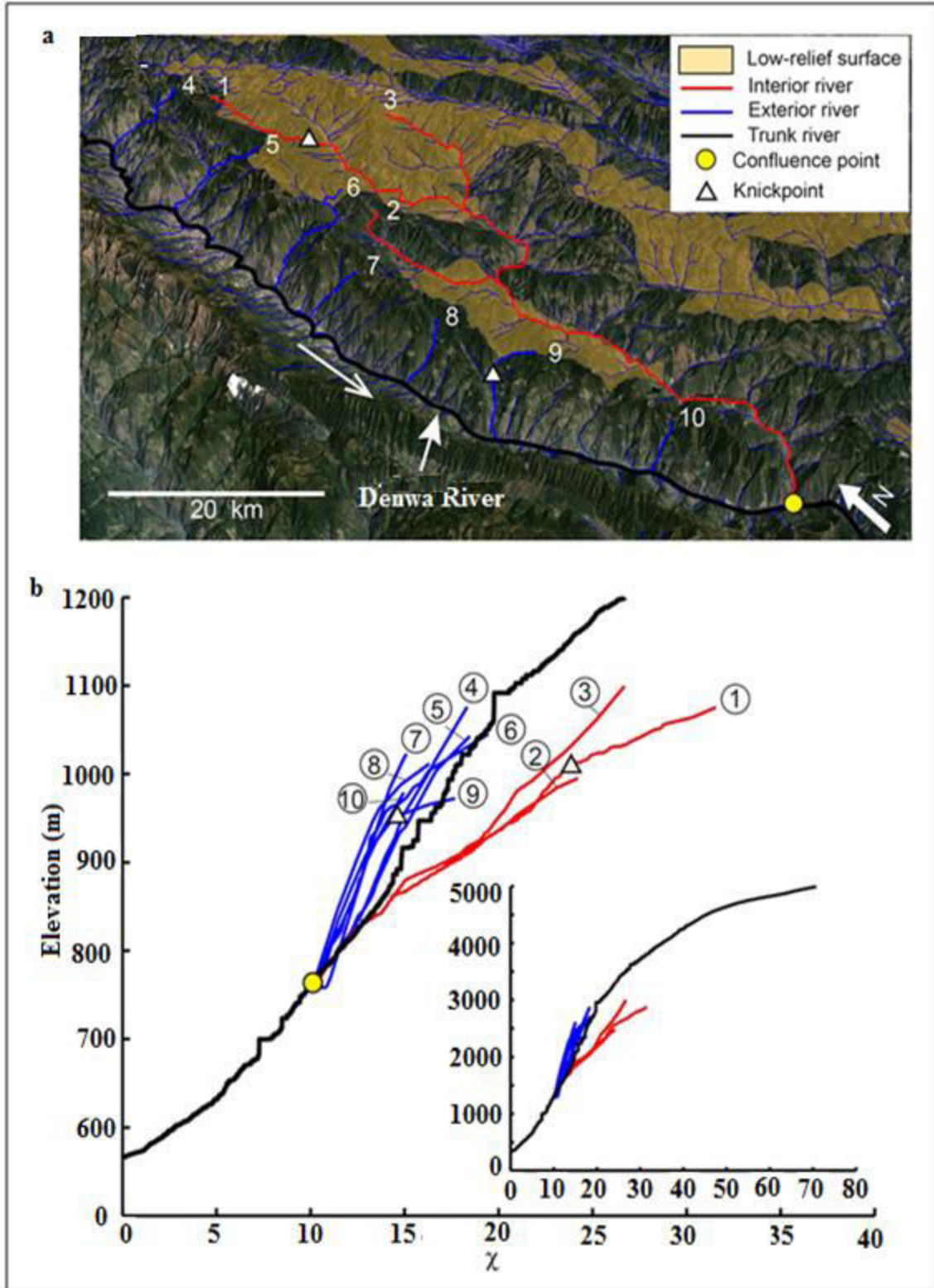


Figure 1: River courses and χ -plots for region of low-relief, 'relict' landscape (Survey of India Toposheet-55J/7) of the Denwa River drainage.

Areas with a linear scaling thus enabling efficient calculation ($O(n)$) at each time step of the simulation even for large grids (Braun and Willett, 2013).

Digital elevation models of real landscapes frequently contain data artifacts that generate topographic sinks. Topographic sinks can also occur as a result of diffusion on hillslopes by creating "colluvial wedges" damming the sections of the river network. By adopting algorithms of flow network derivation from TopoToolbox, top toolbox landscape evolution models makes use of an efficient and accurate technique for 160 drainage enforcement based on auxiliary Topography to derive non-divergent (D8) flow networks (Schwanghart et al., 2013; Soille et al., 2003). Based on the thus derived flow network, topotoolbox landscape evolution models uses downstream minima imposition (Soille et al., 2003) that ensures that downstream pixels in the network have lower or equal elevations than their upstream neighbors.

3.2. Tectonic displacement

We implement Landscape evolution model a 2D version of a flux limiting total volume method to reduce numerical diffusion when simulating tectonic displacements on a regular grid. Equation (1) can be written as a scalar conservation law:

$$Z_t + f(z)_x + f(z)_y = 0 \quad (9)$$

where $f(z) = \mathbf{v}_x z$ and $f(z) = \mathbf{v}_y z$ are the flux functions of the conserved variable z . We refer to the supp Landscape evolution modelary material of Comforts and Govers (2015: Eq. SI 8 - 12) for a derivation of the differential form of Eq. (9) which can be converted to a numerical semi-conservative flux scheme:

$$z_{i,j}^{k+1} = z_{i,j}^k + \frac{\Delta t}{\Delta x} \left[f_{i-\frac{1}{2},j} - f_{i+\frac{1}{2},j} \right] + \frac{\Delta t}{\Delta y} \left[f_{i,j-\frac{1}{2}} - f_{i,j+\frac{1}{2}} \right] \quad (10)$$

where $z_{i,j}^k$ is the elevation of the cell at row i and column j at time $k \times \Delta t$. f represents the numerical approximation of the physical fluxes from Eq. (9). The in- and out coming fluxes are subsequently approximated with a flux limiting upwind method which is total variation diminishing. A total variation diminishing scheme prevents the total variation of the solution to increase in time and hence prevents spurious oscillations that are associated with higher order numerical methods. The use of a flux limiter allows the method to have a hybrid order of accuracy being second order accurate in most cases but shifting to first order accuracy near discontinuities. Hence the total variation diminishing "finite volume method method establishes a compromise between two desirable properties of a numerical method: it achieves a higher order of accuracy than first order schemes while ensuring numerical stability (Harten, 1983). Topotoolbox landscape evolution models use a staggered Cartesian grid for numerical discretization. The data grid points, or elevations from the digital elevation model (z), are considered to represent the center of the computational cells, whereas the velocity fields (\mathbf{v}_x and \mathbf{v}_y) are located at the cell faces. The numerical total variation diminishing fluxes are calculated following Toro (2009):

$$f_{i+\frac{1}{2},j}^{TVD} = f_{i+\frac{1}{2},j}^{LO} + \varphi_{i+\frac{1}{2},j} \left[f_{i+\frac{1}{2},j}^{HI} - f_{i+\frac{1}{2},j}^{LO} \right] \quad (11)$$

where f^{HI} and f^{LO} represent the high and low order fluxes respectively:

$$f_{i+\frac{1}{2},j}^{LO} = a_0 v_{i+\frac{1}{2},j} z_{i,j}^k + a_1 v_{i+\frac{1}{2},j} z_{i,j}^k$$

$$f_{i+\frac{1}{2},j}^{HI} = \beta_0 v_{i+\frac{1}{2},j} z_{i,j}^k + \beta_1 v_{i+\frac{1}{2},j} z_{i,j}^k \quad (12)$$

The low order fluxes are solved with a first order upwind Godunov scheme (1959):

$$a_0 = \frac{1}{2}(1 + \text{sign}(\mathbf{v})) \text{ and } a_1 = \frac{1}{2}(1 - \text{sign}(\mathbf{v})) \quad (13)$$

The high order fluxes are solved with a Lax-Wendroff scheme (1960):

$$\beta_0 = \frac{1}{2}\left(1 + v \frac{\Delta t}{\Delta x}\right) \text{ and } \beta_1 = \frac{1}{2}\left(1 + v \frac{\Delta t}{\Delta x}\right) \quad (14)$$

From Eq. (12), Eq. (13) and Eq. (14) it follows that:

$$f_{i+\frac{1}{2},j}^{LO} = v_{i+\frac{1}{2},j} z_{i,j}^k$$

$$f_{i+\frac{1}{2},j}^{HI} = \frac{1}{2} v_{i+\frac{1}{2},j} (z_{i,j}^k + z_{i+1,j}^k) - \frac{\left(v_{i+\frac{1}{2},j}\right)^2 \Delta t}{2\Delta x} (z_{i+1,j}^k + z_{i,j}^k) \quad (15)$$

$\varphi_{i+\frac{1}{2},j}$ Represents the flux limiter, which is solved with the van Leer scheme (1997):

$$\varphi_{i+\frac{1}{2},j} = \frac{r_{i+\frac{1}{2},j} + \text{abs}\left(\frac{r_{i+\frac{1}{2},j}}{r_{i+\frac{1}{2},j}}\right)}{1 + \text{abs}\left(r_{i+\frac{1}{2},j}\right)} \quad (16)$$

where r is a smoothness index calculated as:

$$r_{i+\frac{1}{2},j} = \frac{z_{i+2,j}^k - z_{i+1,j}^k}{z_{i+1,j}^k - z_{i,j}^k} \quad (17)$$

The overall performance of the total variation diminishing-finite volume method is evaluated by comparing it with the first order accurate upwind Godunov scheme which is not flux limiting Eq. (13). In the remaining part of the text we refer to this scheme as the first order Godunov Method.

3.3. River network updating

Topotoolbox landscape evolution models features a 1D version of the flux limiting total variation diminishing-finite volume method to solve for river incision (Eq. (7)) which written as scalar conservation law is:

$$z_t + f(z)_x = 0 \quad (18)$$

where $f(z)$ represents the flux function of the conserved variable z , representing the channel elevation. The method is similar than the one described in section 3.2 although fluxes are only calculated in one direction. We refer to the Supper Landscape evolution modelary Information provided by Comforts and Govers (2015) for a full derivation of this scheme. In addition, we implement Landscape evolution model a first 195 order explicit and implicit finite difference

methods for the solution of the stream power law detailed in Braun and Willett (2013). Implicit schemes provide stable solutions regardless of the time step considered, a property desired when simulating landscape evolution over long timescales and large spatial domains. An explicit scheme (both finite difference methods and total variation diminishing-finite difference methods), in turn, requires time steps that satisfy the Courant Friedrich Lewy condition (courant-friedrich-lewy):

$$\frac{KA^m \Delta t}{\Delta x} \leq 1 \quad (19)$$

We introduce an inner time step (Δt_{inner}) for the simulation of river uplift and incision to achieve a sufficiently small time step while maintaining an acceptable runtime (Fig. 1). Top toolbox landscape evolution models also allows for inner time steps satisfying the courant-friedrich-lewy criterion if the implicit solution is used. While the implicit solution is unconditionally stable, an inner time allows us to investigate the impact of the length of the time step on model outcomes (see section 5.1.2). Even when the Courant criterion is satisfied, model runs at low spatial resolutions can potentially allow very large time steps. Large time steps could imply a sudden input of vertical uplift in the solution resulting in the generation of artificial shockwaves. Therefore, top toolbox landscape evolution models allows user to set a maximum length of the inner time step (Δt_{max}) which we set by default to 3000 yr.

Regular grids introduce artifacts in the plan form geometry of river networks because local drainage directions are restricted to eight directions (Braun and Sambridge, 1997). Moreover, as the process formulations are deterministic and flow direction algorithms follow a predefined order, Landscape evolution models tend to produce landscapes that are too uniform with respect to slope morphology and river plan form patterns. To overcome this issue, we apply the method of Grimaldi et al. (2005) to explicitly integrate some 210 randomness in the calculation of the value of the drainage area exponent (m) by attributing a variance to m :

$$\text{var}(m) = \frac{\ln\left(1 + \frac{k_1}{k^2}\right)}{(\ln(A))^2} \quad (20)$$

where k_1 and k are proportionality coefficients. We update at each time step a new value of m for each grid cell randomly drawing an error value from the distribution described by Eq. 13 and adding it to the mean value of m .

Another way to add variability in evolving landscapes is to allow the erodibility parameter K , to vary in space, thereby mimicking local, semi-random variations in rock strength. Here, variability on K is simulated by introducing a normally distributed random deviation with a zero mean.

3.4. Hillslope processes

We implement Landscape evolution model linear hillslope diffusion using an efficient Crank-Nicolson scheme (Pelletier, 2008). This scheme is implicit and therefore allows large time steps. Implicit solutions are well suited since the diffusion equation is a parabolic partial differential equation and 220 much less sensitive to numerical diffusion in comparison to the stream power law, which is a hyperbolic partial differential equation.

A numeric solution of the nonlinear hillslope equation is yet more Digital elevation modelandng. The explicit finite difference methods are limited by the maximum length of the

time step at which numerical stability is maintained. Perron (2011) developed Q-imp, an implicit solver that allows increasing the length of the time step by several orders of magnitude. Whereas the per-operation computational cost of this algorithm is higher in comparison to the explicit solution, the overall performance of this method is better than hitherto 225 alternative solutions (Perron, 2011). Q-imp efficiently calculates hillslope diffusion even for high-resolution simulations but is restricted to hillslope below the threshold slope. Therefore, Q-imp must be combined with a hillslope adjustment algorithm.

We assume that hillslopes instantaneously adjust to over steepening along fault scarps and due to river undercutting (Burbank et al., 1996). We refrain from simulating individual landslides although we acknowledge that single high magnitude low frequency events may be relevant at the time scales of our simulations (Korup, 2006). Instead, our approach implicitly accounts for the combined effects of a large number and variety of landslides that effectively adjust slopes to a threshold slope S_c . The threshold slope can be thought of "an average effective angle of internal friction which controls hillslope stability" (Burbank et al., 1996). We implement Landscape evolution model this hillslope adjustment using a modified version of the excess topography algorithm (Blothe et al., 2015). In this algorithm, elevations z at time step $t + 1$ are derived in a way that entails that the absolute local gradient at each grid cell is less or equal than S_c . This is achieved by decreasing elevations at locations i to the minimum elevation of all other locations j to which we add an offset calculated by the Euclidean distance $\|i, j\|$ and S_c

$$Z_i^{t+1} = \min\{Z_j^t + S_c\|i, j\|\} \quad (21)$$

The above equation entails that Z_i^{t+1} at one location depends on all other grid cells and that the algorithm has a time complexity of $O(N^2)$, which would render it unsuitable for frequent updating during landscape evolution model simulations. To avoid an overtly high computational load, we implement Landscape evolution model the algorithm using morphological erosion with a gray-scale structuring Landscape evolution model (see MATLAB function `ordfilt2`), which is a minimum sliding window with additive offsets calculated from the window size and $240 S_c$. This significantly reduces run times as we calculate elevations at one location from the sliding window. Yet, this approach not necessarily removes all gradients greater than S_c . We solve this by calling the algorithm repeatedly until all slope values are equal or less than S_c .

We assume that albeit sediment might be temporarily redeposited in the system, it will be easily evacuated within a relatively short time span due to the unconsolidated nature of the deposits (McGuire and Pelletier, 2016). This assumption is reasonable for rapidly uplifting and eroding mountain belts, but may not be applicable in other environments where mass wasting occurs (Vanmaercke et al., 2014).

3.5. Boundary conditions

Topotoolbox landscape evolution models allow the use of Dirichlet or Neumann boundaries conditions. Alternatively, one can opt for a random disturbance at one or more boundaries of the modelled domain. The latter is especially of useful when simulating strong lateral displacements which may otherwise generate artificially straight river profiles in the direction of the shortening.

4. Experiments

In order to Digital elevation modelonstrate possible applications of topotoolbox landscape evolution models we carry out two series of numerical experiments. We first illustrate

the impact of different hillslope process models on simulated landscape evolution, using a 30 m resolution digital elevation model of the Pachmarhi of India as an example. Second, we investigate the amount of bias and artificial symmetry introduced in the landscape through the use of regular grids.

4.1. Hillslope processes

Top toolbox landscape evolution models allows to simulate hillslope processes assuming (none)-linear slope dependent diffusion with the consideration of a threshold hillslope. Figure 2 illustrates how different hillslope process algorithms affect the evolution of hillslopes in the Pachmarhi of India (Fig. 2a). We assume no tectonic displacement and use standard parameter values for river incision and hillslope diffusion (Table 1) and a threshold slope (S_c) of 1.2 (m/m) when applicable (Fig. 2b). We illustrate model results after 500 ky in Fig. 2c-d using the current topography as the starting condition. Linear diffusion (Eq. (4)) is not capable to keep up with river incision, which results in strongly over steepened hill slopes near the river channels (Fig. 1c and 1g). While higher values for the diffusion coefficient D will eliminate this problem Landscape evolution model (e.g. Braun and Sambridge, 1997) they are incompatible with experimental findings (Roering et al., 1999) and will restrict hillslope to convex upward shapes. The use of non-linear diffusion in combination with a threshold slope results in hillslope similar to those simulated with linear diffusion in combination with a threshold slope. However, for a similar value of D , hilltops become more smoothed assuming non-linear diffusion as sediment fluxes due to diffusive processes now reach higher values when hillslope approach the threshold slope.

4.2. Artificial symmetry

Regular gridded Landscape evolution models may introduce artificial symmetry in evolving landscapes (Braun and Sambridge, 1997). We perform simulations with an entirely flat initial surface as well as with a random initial surface with uniformly distributed elevations between 0 and 50 m to investigate how random perturbations of the values of m or K affect drainage network evolution we consider four different scenarios for each initial surface (Fig. 3). Scenario 1 is the reference simulation, with a low spatial resolution of 1000 m, a large time step of 5×10^4 years and a K value of $6 \times 10^6 \text{ m}^{-0.1} \text{ yr}^{-1}$. In scenario 2, the mean erodibility K is halved. In scenario 3 the time step is set to 1×10^4 years while in scenario 4, the spatial resolution is set to 200 m.

At low spatial and temporal resolutions, the use of uniform parameter values results in clear artificial symmetry (Fig. 3). Introduction of random variability on m mainly decreases similarity close to the river heads where the drainage areas are the smallest (scenario 1). This is a consequence of the formulation of Eq. (20): the introduced variability is relatively larger for small catchments. Variability in K slightly decreases overall artificial symmetry at low spatial resolutions (senario1). The use of a lower (mean) K value, representing slower river incision also decreases overall artificial symmetry (scenario 2). Decreasing the time step (scenario 3) results in slightly different drainage networks in comparison to simulations with larger time steps but fails to reduce the symmetry in the result. At a high spatial resolution (scenario 4), artificial symmetry is still present when constant parameter values are used. However, inserting variability on the m and K parameters is much more effective in reducing symmetry at this resolution.

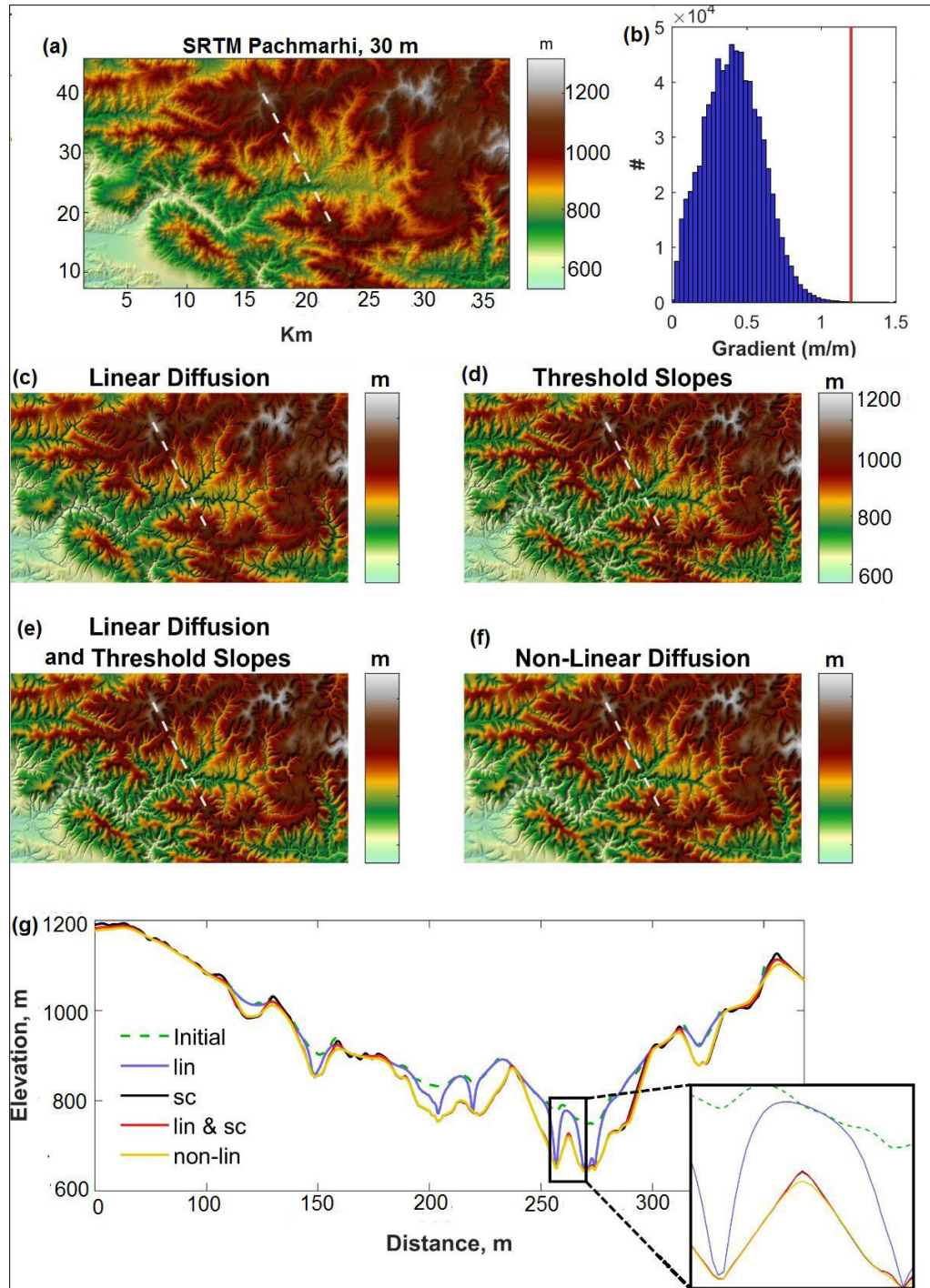


Figure 2. Hillslope response to river incision. (a) Standard srtm digital elevation model (30 m) included in TopoToolbox representing the Pachmarhi region. The dotted grey line indicates the location of the transect shown in subplot g. (b) Resulting topography after k years using four different descriptions for hillslope evolution. (c) Linear diffusion over all slope values (lin). Threshold landscape where no slopes exceed the threshold slope (S_c). (e) Linear diffusion 695 combined with immediate adjustment to a threshold slope (S_c). (f) Non-linear diffusion combined with immediate adjustment to a threshold slope (S_c). (g) Elevation profiles of the different model runs compared with the initial profile. Model parameter values are listed in Table1.

Table 1. Model parameters used for the topotoolbox landscape evolution models simulations.

| Parameter | Units | Figure 2 | Figure 3 | Figure 4 | Figure 5 | Figure 7-9 |
|---------------------------------|--------------------|----------------------|---|--------------------------|-----------------------|---|
| <i>Initialization</i> | | | | | | |
| Initial Surface | | Pachmarhi | flat - random | flat, 1D | random | synthetically produce digital elevation models shown in Fig.3 |
| Uplift Pattern | | | uniform | variable in time | uniform | uniform |
| Uplift Rate | m yr ⁻¹ | 0 | 1 × 10 ⁻³ | 0 - 1 × 10 ⁻³ | 1 × 10 ⁻³ | 0 - 3 × 10 ⁻³ |
| Spatial Step | m | 30 | 200 - 1000 | 100 | 100 | 100 - 500 |
| <i>Computational parameters</i> | | | | | | |
| Time Span | yr | 5 × 10 ⁵ | 50 × 10 ⁶ | 1 × 10 ⁶ | 150 × 10 ⁶ | 5 × 10 ⁶ |
| Time Step | yr | 1250 | 1 × 10 ⁴ - 5 × 10 ⁴ | ca. 5 × 10 ³ | 1 × 10 ⁵ | 5 × 10 ⁴ |
| Area Thresh | m ² | 2 × 10 ⁵ | 2 × 10 ⁶ | - | 2 × 10 ⁵ | 2 × 10 ⁵ |
| DrainDir | | variable | variable | - | variable | |
| DiffToRiv | | FALSE | FALSE | - | FALSE | |
| steadyState | | FALSE | TRUE | - | TRUE | |
| SS_Value | m | | 5 | - | 0.5 | |
| parallel | | FALSE | FALSE | - | FALSE | |
| massWasting_river | | FALSE | FALSE | - | FALSE | |
| <i>Boundary conditions</i> | | | | | | |
| BC_Type | | Neumann | Dirichlet_Matrx_Ini | - | Dirichlet | - |
| BC_dir_DistSites | | - | - | - | - | - |
| BC_dir_Dist_Value | | 1 | 1 | - | 1 | - |
| BC_dir_value | | 0 | 0 | - | 0 | - |
| BC_nbGhost | | 1 | 1 | - | 1 | - |
| FlowBC | | - | - | - | - | - |
| <i>River incision</i> | | | | | | |
| Kw | $L^{1-2m} t^{-1}$ | 4 × 10 ⁻⁶ | 6 × 10 ⁻⁶ - 3 × 10 ⁻⁶ | 5 × 10 ⁻⁶ | 5 × 10 ⁻⁶ | 5 × 10 ⁻⁶ |
| m | | 0.45 | 0.45 | 0.42 | 0.45 | 0.45 |
| n | | 1 | 1 | 1 | 1 | 1 |
| m_var | | 0 | 0 - 0.2 | - | 0 | - |
| | | | 0 | | - | |
| K_weight | - | - | - | - | - | - |
| | | | normally distributed | | | |

| | | | | | | |
|---|---------------------------------|--|---|-----|--|--|
| Norm Precip | - | - | - | - | - | - |
| Hillslope response | | | | | | |
| D | m ² yr ⁻¹ | 0.015 | 0.036 | - | 0.036 | 0.03 |
| $\rho r \rho s^{-1}$ | - | 1.3 | 1.3 | 1.3 | 1.3 | 6 |
| DiffTol | | 1×10^{-4} | 1×10^{-4} | - | 5×10^{-4} | 1×10^{-4} |
| Sc | m m ⁻¹ | 1.2 | 0.7 | - | 0.7 | 1 |
| Sc_unit | | tangent | tangent | - | tangent | |
| Tectonic shortening | | | | | | |
| shortening | | FALSE | FALSE | - | FALSE | |
| short_x | m yr ⁻¹ | | | | | |
| short_y | m yr ⁻¹ | | | | | |
| Numerics | | | | | | |
| riverInc | | implicit finite difference methods | implicit finite difference methods implicit finite difference methods total variation diminishing finite volume method | | implicit finite difference methods | implicit finite difference methods total variation diminishing finite volume method |
| Courant- Friedrich- Lewys diffScheme | | 0.7 | 0.7 | 0.7 | 0.7 | 0.7 |
| shortening_meth | | imp_lin only_sc imp_lin_sc c imp_nonli n_sc | imp_lin_sc | - | imp_lin_sc | |
| | | Upwind_t otal variation diminishin g | Upwind_total variation diminishing | - | Upwind_total variation diminishing | |
| Model output | | | | | | |
| ploteach | | 1 | 1 | - | 1 | 0 |
| saveeach | | 1 | 1 | - | 1 | 0 |
| fileprefix | | res_ | ArtSym_RandI ni_1_Si mNb_1_ | - | standard_run _1 00m | - |
| resultsdir | | C:\DATA ... | C:\DATA_.. . | - | C:\DATA_ ... | - |

Drainage networks simulated using an initial surface with elevations that randomly vary between 0 and 50 m are almost free of artificial symmetry and the final geometry of the drainage

network is now less dependent of parameter variability. The latter underscores the importance of initial digital elevation model conditions for the final results of a simulation (Perron and Fagherazzi, 2011). Nonetheless, even with a randomly varying initial surface, the perturbation on parameter values clearly affects the drainage network that is produced. Parameter value perturbation generally results in drainage networks which are less rectilinear than those simulated without perturbation.

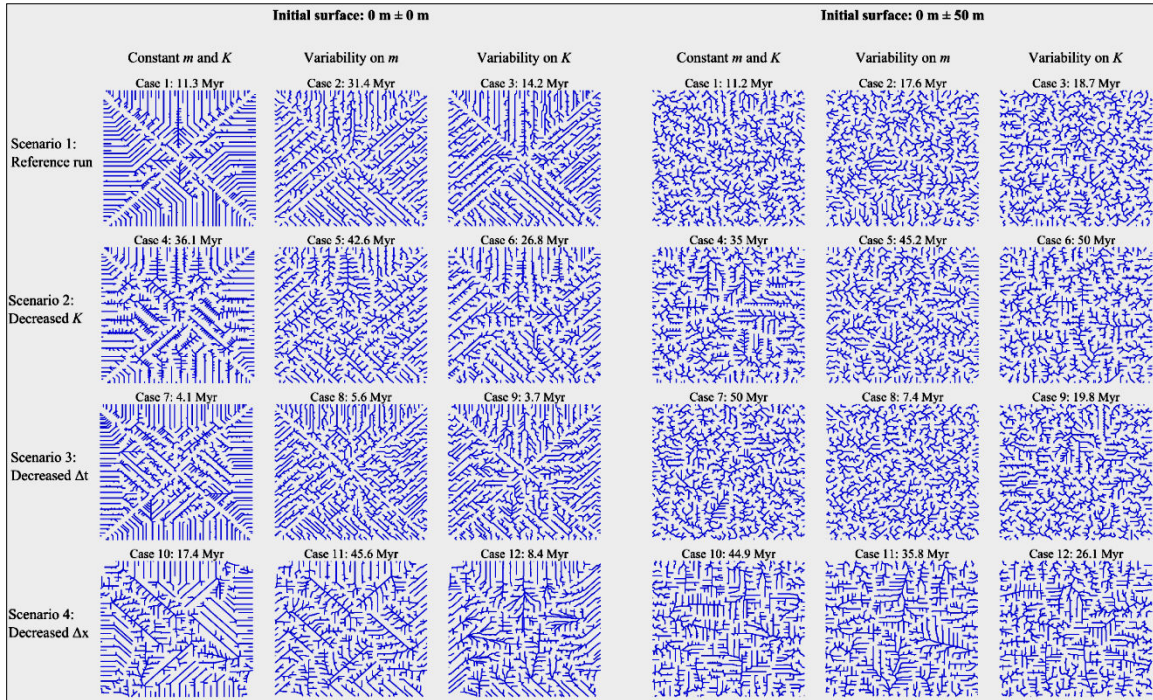


Figure 3. Steady state river networks obtained with different model configurations. The age at which 700 a steady state is achieved is given in the title of the subplot. The first three columns in the left hand side of the figure represent model runs initiated from a flat, zero elevation surfaces. The first three columns in the right hand side of the figure represent model runs initiated from a surface with elevations randomly varying between 0 and 50 m. The configuration of the different model simulations is explained in the text and parameter values are listed in Table 1.

5. Impact of numerical methods

In a next step we investigate to what extent the numerical schemes implement Landscape evolution modeled in topotoolbox landscape evolution models affect simulated landscape evolution. We distinguish between the effects on simulated river incision on the one hand and on simulated tectonic displacement on the other. We use a synthetically generated landscape for all simulations as a starting condition because we are interested in the evaluation of the functionality of the model and not on the correct simulation of the evolution of a particular landscape or region. Hence, our simulations are uncelebrated and results were not compared with a 'true' landscape: however, the chosen parameter values are realistic.

5.1. River incision

5.1.1. 1D River incision

The impact of numerical diffusion on propagating river profile knickpoints is most obvious in situations where an analytical solution is available. The first simulation illustrates such

a situation, with an artificial river profile characterized by a major knickzone between 8 and 12 km from the river head (Fig. 4). We assume that the drainage area is increasing in proportion to the square of the distance and uplift equals zero. For this simple configuration, an analytical solution for the SPL can be found using the method of characteristics (Luke, 1972). Notwithstanding the relatively high spatial resolution of 100 m, both implicit and explicit Finite Difference Methods (finite difference methods) suffer from clear numerical diffusion when river incision is calculated over a time span of 1 Myr (Fig. 4). The total variation diminishing-finite volume method achieves a much higher accuracy, a finding that is systematic, occurring over a wide range of spatial resolutions and parameter values (Campforts and Govers, 2015).

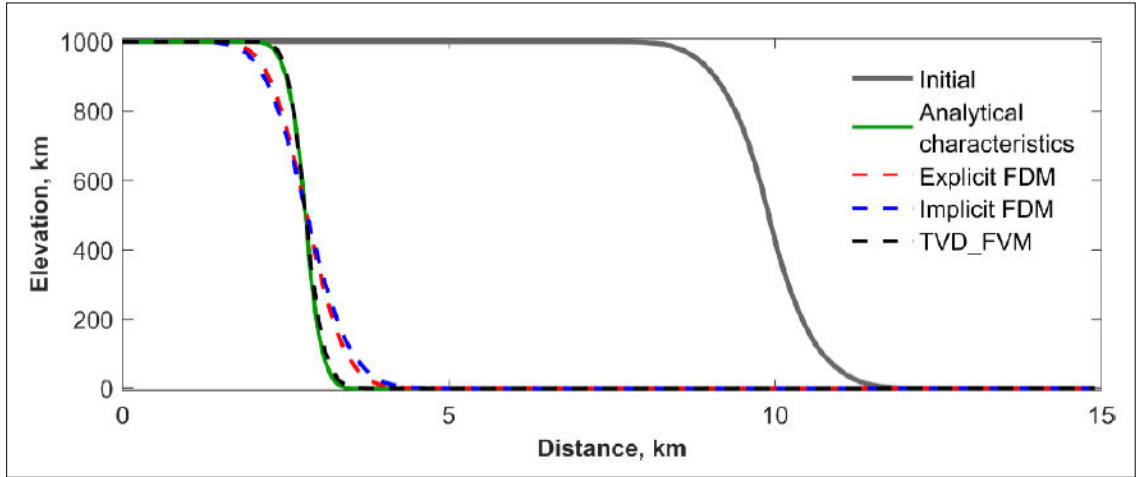


Figure 4. Solution of the linear 1D stream power law for a synthetic knick zone over a time span 710 of 1 Myr. The analytical solution is obtained with the method of characteristics. The spatial resolution equals 100 m. Other model parameter values are listed in Table 1.

5. 1. 2. River incision and catchment wide erosion rates

We hypothesize that apart from river profile evolution, the accurate simulation of river knickpoints will influence landscape evolution as a whole. In order to investigate the sensitivity of catchment wide erosion rates to different numerical schemes of the river incision model, we first create a steady-state artificial landscape that we initialize with uniformly distributed random elevation values between 0 and 50 m on a 50 km x 100 km grid with a spatial resolution of 100 m. Landscape evolution is simulated using Dirichlet boundary conditions and by inserting spatially and temporally uniform vertical uplift of 1 km Myr^{-1} over a period of 150 Myr. Outer model time steps are set to $5 \times 10^4 \text{ yr}$. Parameter values for river incision and hillslope response are constant in space and time and are reported in Table 1. Figure 5 shows the resulting steady state landscape.

We impose four consecutive uplift pulses of equal magnitude to this artificial landscape (Fig. 5). Uplift pulses have a wavelength of 1.25 Myr and amplitude of $1.5 \times 10^{-3} \text{ m yr}^{-1}$ (Fig. 6). Top toolbox landscape evolution models is run over 5 Myr with main model time steps of $5 \times 10^4 \text{ yr}$, again with Dirichlet boundary conditions and plan form fixed drainage network. We use two spatial resolutions (100 m and 500 m) and three different numerical methods (implicit finite difference methods without time step limitation, implicit finite difference methods with time step limitation (courant-friedrich-lewy condition applied) and total variation diminishing-finite volume method) to simulate river incision. When applicable, the length of the inner time step is set to $3 \times 10^3 \text{ yr}$. Without inner time steps, river incision is calculated once for each main (outer) model time step ($5 \times 10^4 \text{ yr}$).

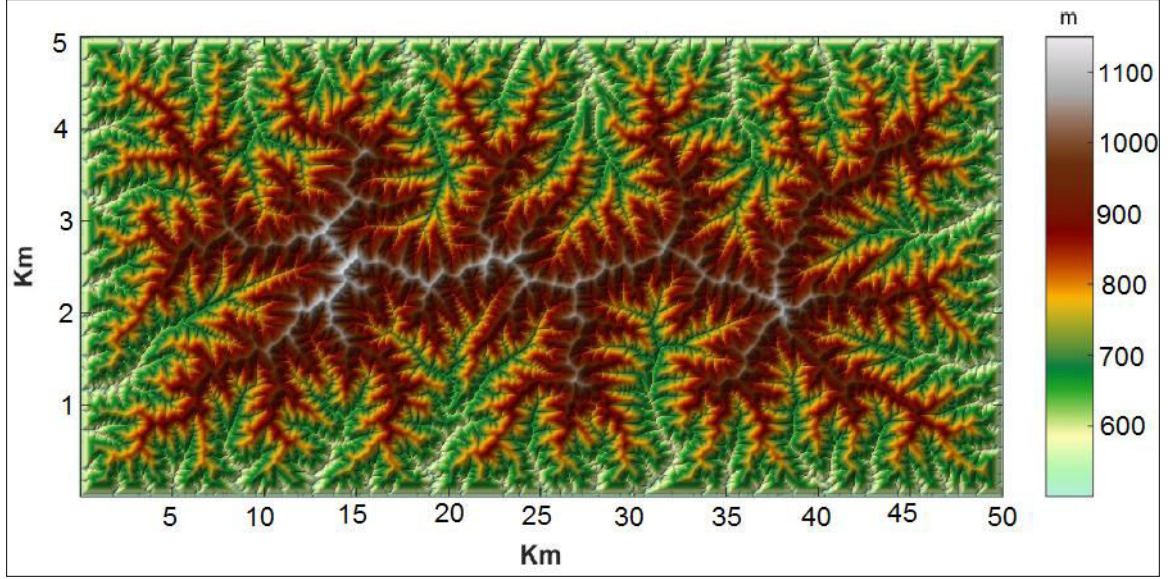


Figure 5. A synthetic steady state landscape produced as the testing environment to verify and compare 715 the different numerical schemes implement Landscape evolution modulated in topotoolbox landscape evolution models. Model runtime was 150 Myr, uplift rate was assumed to be spatially uniform over the area (block uplift) and fixed to 10-3 m yr-1. Other model parameter values are listed in Table 1.

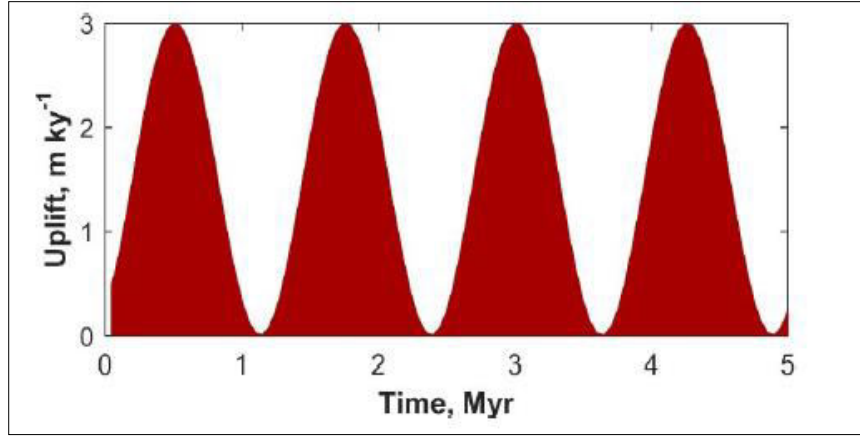


Figure 6. Uplift imposed to the steady state landscape show in Figure 5 to investigate the impact of different numerical schemes.

We compare differences in simulated erosion rates by randomly selecting a number of catchments with drainage areas ranging 325 between 1 and 50 km² (221 and 202 catchments for runs at a spatial resolution of 100 m and 500 m respectively) (Fig.8). We calculate the erosion rates for each time step by subtracting the elevation grid in the previous time step from the updated, current, elevation grid. The difference between the results obtained with different numerical schemes is quantified by calculating a Root Mean Square Error:

$$\text{Root Mean Square Error} = \sqrt{\frac{\sum_{i=1}^n (\varepsilon_{iTVD} - \varepsilon_{iFDM})^2}{nd}} \quad (22)$$

where $\varepsilon_{i,TVD}$ and $\varepsilon_{i,FDM}$ refer to the catchment wide erosion rates simulated with the total variation diminishing-finite volume method and finite difference methods respectively to simulate river incision and n_b is the total number of discrete time steps of the simulated erosion record.

We rank the catchments from low to high Root Mean Square Error for each comparison to investigate overall variations in catchment wide erosion rates. Figure 7 shows the results for the catchments at 10%, 50% (median) and 90% percentile. Note that the ranking is performed separately for the models runs at 100 m and 500 m as different sub catchments are randomly generated for both 335 simulation runs. The percentiles shown in Fig. 7 therefore represent different catchments.

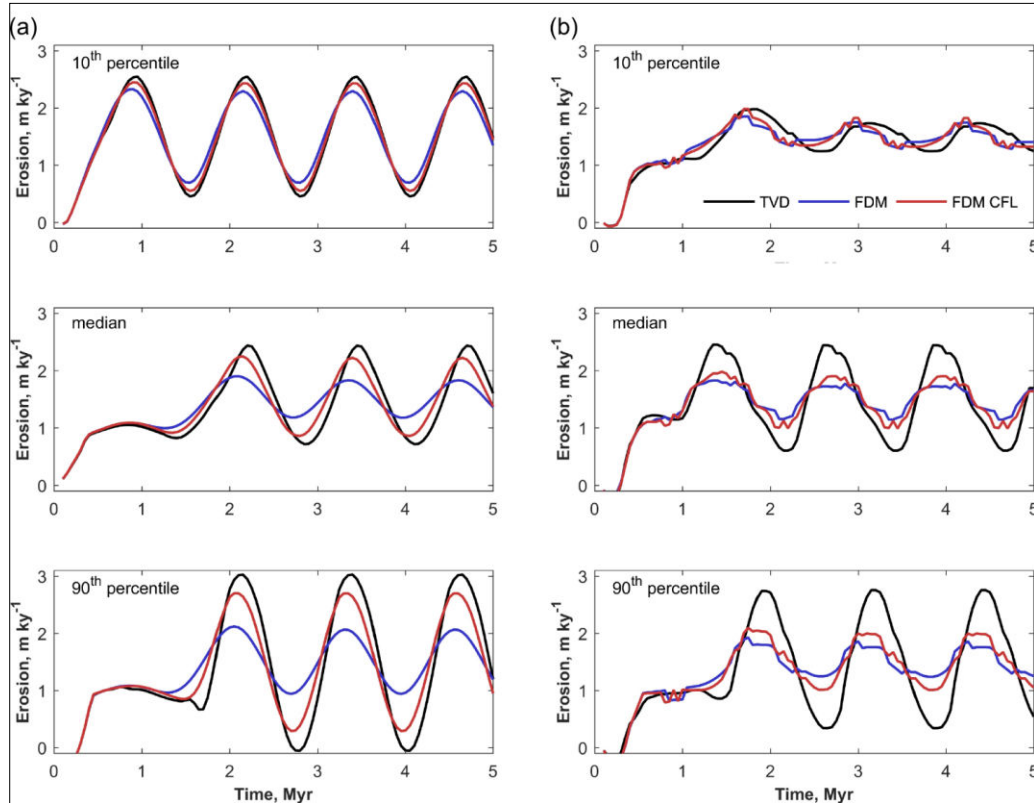


Figure 7. Temporal variation in simulated catchment wide erosion rates using different numerical methods to simulate river incision. The black lines represent simulations where a flux limiting total variation diminishing-finite volume method is used, the blue lines represent the implicit finite difference methods without constraints on the time steps and the red lines represent the finite difference methods with an inner time step calculated with the courant-friedrich-lewy criterion. (a) Simulations performed at a spatial resolution of 100 m. (b) Simulations performed at a spatial resolution of 500 m. Here, a median filter with a window of 3 time steps was applied on the simulated erosion rates to eliminate spikes which might occur at low resolutions.

For most catchments, we observe significant differences in erosion response between the three numerical methods at a spatial resolution of 100 m. The amplitude of the response to a tectonic uplift pulse increases when reducing numerical diffusion: the use of a first order implicit finite difference method without time step restriction results in a much smoother response in comparison to the total variation diminishing-finite volume method. The variations in response amplitude are significant: the majority of the catchments record amplitude reductions by 340

more 50% when model with the implicit finite difference methods without time step restriction. Time step restriction (and thereby sacrificing the main advantage of the implicit finite difference methods) significantly reduces numerical diffusion so that most catchments display an erosional response comparable to that simulated by the total variation diminishing-finite volume method. However, this finding is supported only by the simulation with 100 m spatial resolution. The advantage of a time step restricted implicit finite difference methods over a non-restricted implicit finite difference methods disappears almost completely for a coarser grid resolution of 500 m.

Catchment-wide erosion rates vary systematically with the use of different numerical methods. Figure 8 shows that erosion rates diverge between the different methods with increasing distance to the outlet of the main river while they are similar for larger catchments. A smaller effect of the numerical scheme on large catchment areas may be partly due to stronger averaging of local variations in catchments. In addition, catchments at a large distance from the outlet—and thus likely with smaller catchment areas—tend to experience the uplift signal only after several model time steps. If catchments are far from the fault zone, knick points will then be significantly smoothed if an implicit finite difference methods is used, which will affect the response of the catchment. This smoothing is not apparent if the catchment is close to the border of the modelling domain. Again, spatial resolution matters: a larger grid size not only results in larger differences on average but also in larger differences between small and large catchments (Fig. 8).

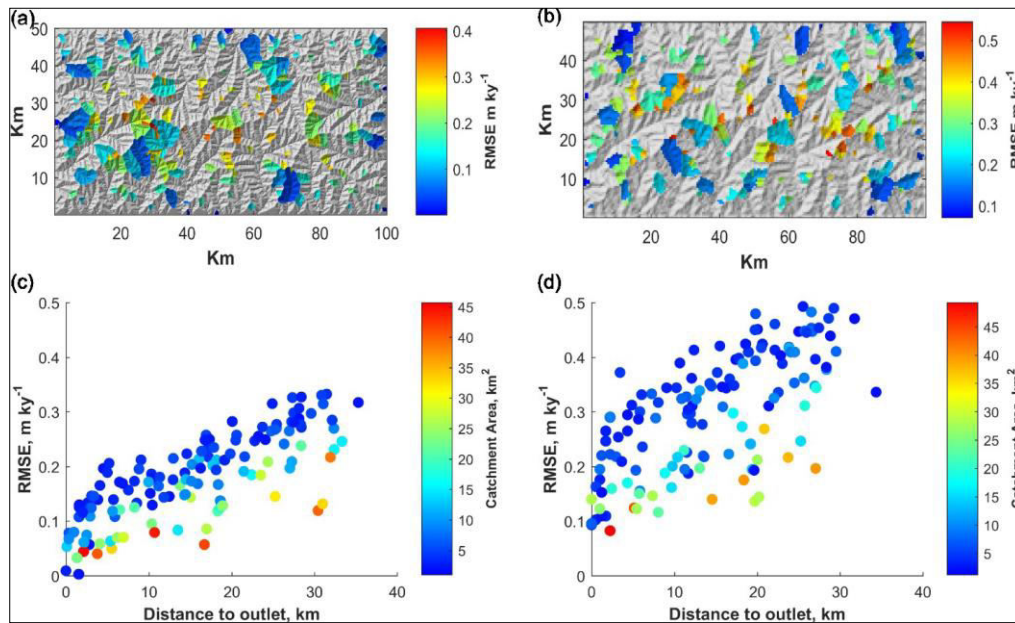


Figure 8. Spatial variation of differences between simulated erosion rates calculated with a flux limiting total variation diminishing-finite volume method for simulating river incision and an implicit finite difference method. Here, we compare methods both run with an inner timestep constrained with the courant-friedrich-lewy criterion (see text). Root Mean Square Error is thus calculated between the black and red lines from Figure 7. Left column represents simulations run at a spatial resolution of 100 m, right column at 500 m. (a and b) Location of the randomly selected catchments with an area $> 1 \text{ km}^2$ and $< 50 \text{ km}^2$. Colors refer to the Root Mean Square Error between the two simulations. (c and d) Differences between the schemes increase with increasing distance from the river outlets and are inversely correlated with the catchment area.

The differences in catchment response relate to the differences in simulated erosion rates within the catchments. Figure 9 illustrates the spatial difference in erosion rates calculated with

the two numerical methods during the final step of the model run (after 5 Myr). This figure shows that spatial differences are significant and form a systematic banded pattern related to the upslope migration of the erosion waves of the individual uplift pulses.

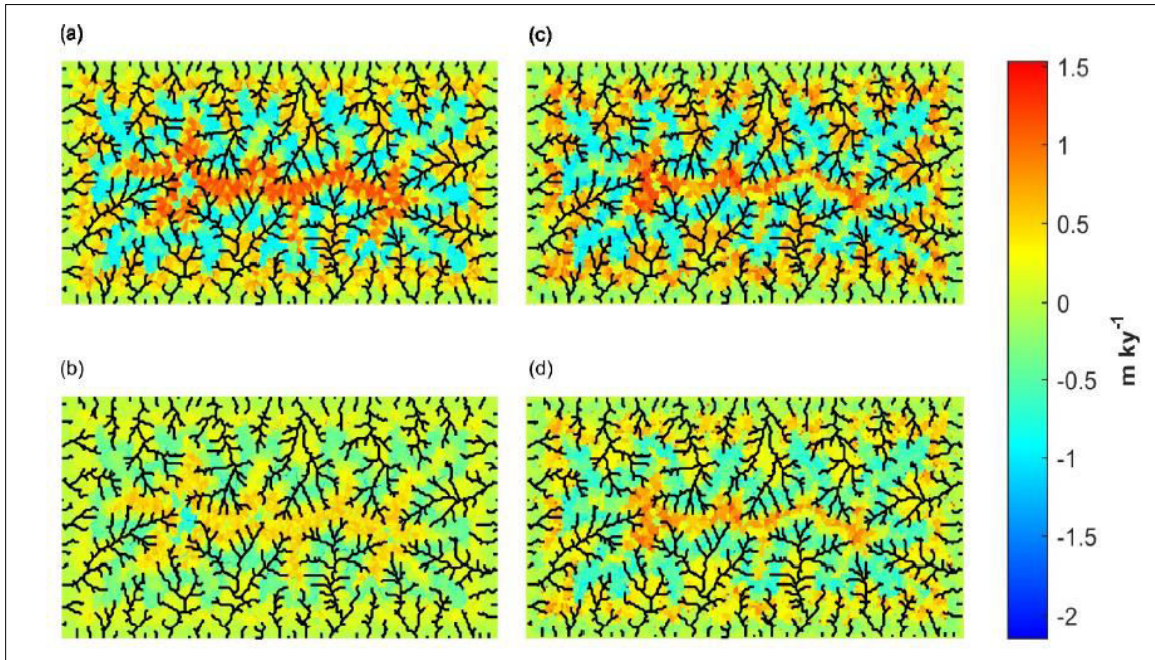


Figure 9. Spatial pattern of erosion rates during one model time step when simulating landscape evolution with the flux limiting total variation diminishing-finite volume method versus the first order implicit finite difference methods. (a) simulation at a resolution of 100 m where 740 the time step of the implicit method is not constrained (b) simulation at a resolution of 100 m where the time step of the implicit method is constrained with the courant-friedrich-lewy criterion (c) simulation at a resolution of 500 m where the time step of the implicit method is not constrained (d) simulation at a resolution of 500 m where the time step of the implicit method is constrained with the courant-friedrich-lewy criterion.

5.2. Tectonic displacement

We test the performance of the 2D version of the flux limiting total variation diminishing-finite volume method to simulate tectonic displacement using a simplified model setup. We use a synthetic landscape as an initial condition and impose a constant lateral tectonic displacement while keeping erosion rates zero. Theoretically, this should result in a laterally displaced landscape that, apart from this, remains unchanged in comparison to the initial state. We compare the flux limiting total variation diminishing-finite volume method with a first order accurate upwind Godunov Method Figure 10 illustrates the results when applying a tectonic displacement in two directions ($v_x = v_y = 10 \text{ mm yr}^{-1}$) over a time span of 1 Myr. The results show that the explicit Godunov method strongly smoothes the resulting digital elevation model whereas the 2D total variation diminishing-finite volume method scheme produces a digital elevation model that is very similar to the initial digital elevation model, with minimal amounts of numerical diffusion.

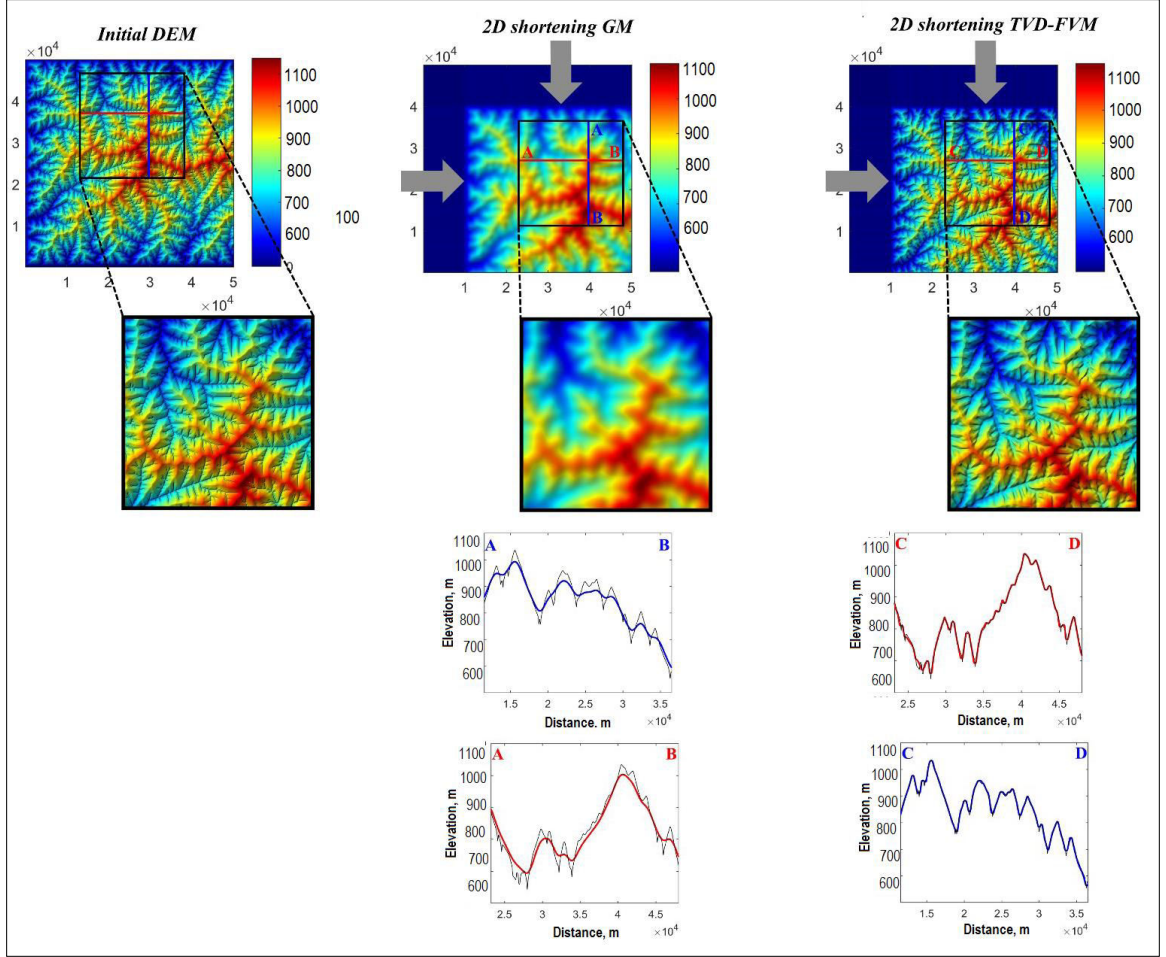


Figure 10. Impact of numerical schemes when simulating horizontal shortening on a fixed grid. Left: extract from synthetically produced digital elevation model from Fig. 5. Middle: horizontal shortening in two directions simulated with a 2D explicit first order Godunov Method . Right: horizontal shortening in two directions simulated with a 2D explicit flux limiting total variation diminishing-finite volume method.

In order to quantify and better understand the amount of numerical diffusion ($DN [L^2 yr^{-1}]$) introduced by the Godunov method and the total variation diminishing-finite volume method, we test a range of different model configurations and calculate the numerical diffusivity, D_N , corresponding to the observed smoothing. The latter is done by calculating the diffusivity required to transform the initial digital elevation model DEM_{ini} to the 370 final digital elevation models produced at the end of the simulations (DEM_{funt}). the optimum amount of diffusion is determined by minimizing the misfit function H with a sequential quadratic programming method (Nocedal and Wright, 1999). H is given by:

$$H = \sqrt{(DEM_{inu} - DEM_{funt})^2} \quad (23)$$

Figure 11.a illustrates the relation between D_n and the spatial resolution of different numerical approximations. The 2D total variation diminishing-finite volume method decreases numerical diffusion by a factor of 5-60 compared to the Godunov method (Fig. 11b). The accuracy increases for both schemes with increasing resolution and increasing courant-friedrich-lewy numbers. The

increase in accuracy with higher spatial resolution is due to smaller spatial steps that result in better approximations of the spatial derivatives. Yet, the gain in accuracy with increasing spatial resolution is higher for the total variation diminishing-finite volume method than for the Godunov method. Our analysis shows that the explicit finite difference methods

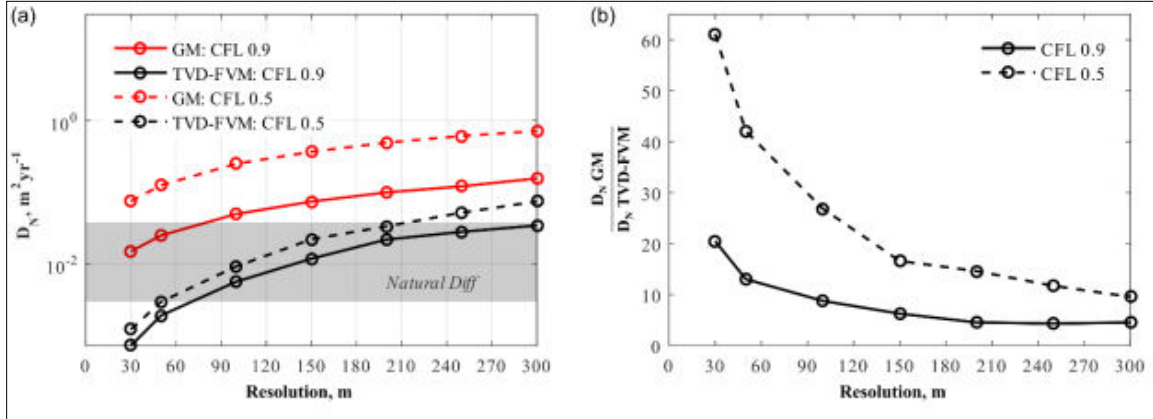


Figure 11. (a) Amount of numerical diffusion (DN) introduced in the system when simulating lateral tectonic displacement in two directions as a function of raster resolution. The grey zone indicates the range of naturally observed diffusion rates. (b) The ratio between the amounts of numerical diffusion for the first order Godunov Method versus the flux limiting total variation diminishing finite volume method.

Performs best with a courant-friedrich-lewy criterion close to one. This may seem counterintuitive as one might expect smaller time steps (courant-friedrich-lewy = 0.5) to lead to higher accuracies. However, the accuracy gain from an increase in temporal resolution is reduced by additional numerical diffusion that is introduced by more iterations within a given time interval (Gulliver, 2007).

6. Discussion

There is a growing consensus that most eroding landscapes are in a transient state (Mudd, 2016; Vanacker et al., 2015). Landscape evolution models with high numerical accuracy are thus needed to capture transiency correctly, yet most commonly applied first order accurate numerical methods introduce numerical diffusion and smear discontinuities that are inherent in transient landscapes. Knick points in river systems are of particular concern to geomorphologists as their analysis reveals insights into the tectonic and climatic controls on evolving landscapes. However, no analytical solution exists that allows simulating river incision for changing drainage areas (Fox et al., 2014). Because drainage networks and drainage divides evolve in dynamic ways (Willett et al., 2014), the analysis of transient landscapes must thus rely on numerical methods, although analytical models can be applied in specific cases (Perron and Royden, 2013). We present a higher order flux limiting scheme (referred to as total variation diminishing-finite volume method) that overcomes this problem Landscape evolution model of numerical diffusion.

Our simulations show that optimizing numerical schemes of Landscape evolution models is far from being only a numerical exercise. The impact of the numerical scheme to simulate detachment limited river incision on model outcomes is substantial and not limited to river profile development alone. Hillslopes adjust to local base level changes dictated by river incision. Hillslope denudation rates 395 must thus —at least partly— reflect the geometry of a knickpoint, whether it is a diffuse signal or a sharp discontinuity migrating upstream. Our simulations show that depending on the spatial and temporal resolution, catchment wide erosion rates are more

responsive to uplift when derived from the total variation diminishing-finite volume method in comparison to finite difference methods. First order (explicit and implicit)

Finite difference methods fail to properly reproduce transient incision waves (Campforts and Govers, 2015; Pelletier, 2008) with the effect that the smoothing propagates to inferred rates of hillslope denudation and that catchment wide erosion rates are smeared over geological time. Thus, the use of a shock preserving method such as total variation diminishing-finite volume method is strongly recommended for accurate simulations of transient landscapes.

It could be argued that TOTAL variation diminishing-finite volume methods are unnecessary as long as one applies an implicit method in combination with a sufficiently small time step. Although small time steps partly resolve the problem Landscape evolution model of smearing, their effect on numerical accuracy can hardly be generalized. Our simulations show that, for the selected parameter value combinations, results were only acceptable if a time step restriction is combined with a relatively high spatial resolution (100 m). In addition, it is well possible that, for other parameter value sets, numerical diffusion will be important, even if a fine grid is used. It would be infeasible for a model user to detect smearing problem Landscape evolution models in standard applications as comparable exact, analytically derived solutions, usually are nonexistent. Hence, we argue that the use of a shock capturing total variation diminishing-finite volume method numerical scheme is preferable since it avoids significant numerical diffusion under a wide range of parameter values and spatial resolutions. Moreover, by constraining the time step of a first order implicit method below the Courant-Friedrich-Lewy criterion, the main advantage of an implicit scheme, i.e., the stability for any time step, disappears.

One might debate the significance and necessity of numerical schemes that avoid diffusion of retreating knick points. We think that it is critical to simulate knick point retreat using a method that avoids numerical diffusion. Even in bedrock-dominated landscapes knick zones are often smoothed, possibly due to flow acceleration above knick zone lips and subsequent localized higher erosion (Berlin and Anderson, 2007). The discrepancy between actual and simulated longitudinal profiles of hanging valleys has prompted (Valla et al., 2010) to prefer a transport-limited model (Willgoose et al., 1991a) over a detachment-limited model (Howard, 1994; Whipple and Tucker, 1999). The presence of significant sediment loads does not necessarily imply that transport limitations control river incision. Sediment flux dependent models, as first proposed by Sklar and Dietrich (1998) consider the hybrid role of sediment particles, acting as a tool to break and erode river beds in eroding regimes and as a covering armor in depositional regions (Gasparini and Brandon, 2011; Sklar et al., 1998). One-dimensional analytical simulations have shown that this process might generate over-steepened river reaches and explain the presence of permanent hanging fluvial valleys (Crosby et al., 2007). Numerical Landscape evolution models accounting for saltation-abrasion have so far not been able to reproduce such permanent hanging valleys: however this may be caused by the effects of numerical diffusion rather than by an inadequate process formulation (Crosby et al., 2007). Simulation of sharp knickpoints is also required in geomorphological and lithological settings where knickpoint retreat is caused by rock toppling, possibly triggered during extreme flood events, where knickpoint diffusion through abrasion and plucking of small blocks is minor (Baynes et al., 2015; Lamb et al., 2014; Mackey et al., 2014). Thus, various scenarios of knickpoint retreat exist, some which are characterized by significant natural diffusion, while others are not. In both cases simulation tools with a minimum of numerical diffusion are required to correctly quantify the importance natural diffusion.

First order numerical methods also inadequately simulate tectonic displacement on a regular grid. The amount of numerical diffusion that is introduced by these methods will, in many cases, far exceed natural diffusion rates, thus rendering accurate simulation of hillslope development impossible. A 2D variant of the total variation diminishing-finite volume method, instead, strongly reduces the amount of numerical diffusion to values well below natural diffusivity values, an effect that is especially apparent at high spatial resolutions. We thus implement Landscape evolution modeled a scheme that allows to accurately model a process that significantly impacts the evolution of topography and river networks (Willet, 1999), but whose simulation was hitherto mainly restricted to Landscape evolution models with flexible spatial discretization schemes.

Although most Landscape evolution models use first order accurate discretization schemes (Valters, 2016), the problem Landscape evolution model of numerical diffusion has been widely discussed in the broader geophysical community (Durran, 2010; Gerya, 2010). An alternative family of shock capturing Eulerian methods being frequently applied is the MPDATA advection schemes (Jaruga et al., 2015). These schemes are based on a two-step approach in which the solution is first approximated with a first order upwind numerical scheme and then corrected by adding an anti diffusion term (Pelletier, 2008). However, contrary to the total variation diminishing-finite volume method, the standard MPDATA scheme (Smolarkiewicz, 1983) is not monotonicity preserving (or is not total variation diminishing). Instead, MPDATA introduces dispersive oscillations in the solution if combined with a source term (such as uplift) in the equation (Durran, 2010). Adding limiters to the solution of the anti diffusive step (Smolarkiewicz and Grabowski, 1990) renders the MPDATA scheme oscillation free (Jaruga et al., 2015). However, by adding this additional correction, the method approaches the numerical nature of the total variation diminishing-finite volume method which does not require further adjustments in any case. Lagrangian schemes offer another alternative and are based on so called markers which evolve with the changing variable over time (Gerya, 2010). In the framework of a raster-based landscape evolution model, a fully Lagrangian tracing scheme is not desired and can be replaced by semi-Lagrangian methods that require interpolation between the propagating markers and the grid cells (Spiegelman and Katz, 2006). These methods could potentially achieve high accuracy. However, simulation of horizontal topographic shortening would require large amounts of incremental markers to prevent numerical diffusion when interpolating the solution to the grid used in topotoolbox landscape evolution models. Both memory requirements and interpolation processing times therefore legitimize the use of the total variation diminishing-finite volume method which is sufficiently accurate and avoids interpolation.

Some of the weaknesses of the tested numerical solutions can be reduced by Landscape evolution models that rely on irregular grid geometries. A Topotoolbox landscape evolution model avoids these techniques but rather attempts to run on rectangular grids with a maximum of accuracy. We chose so for several reasons: First, input data such as topography, climate, lithology or tectonic displacement fields are typically available as raster datasets and thus require only minor modifications whereas irregular grids require substantial preprocessing. Second, topotoolbox landscape evolution models output can instantly be analyzed and visualized using the Topo Toolbox library (Schwanghart and Kuhn, 2010; Schwanghart and Scherler, 2014) or any other geographic information system. Thus, while irregular grid geometries and flexible grids may have some advantages over rectangular grids with respect to numerical accuracy, topotoolbox landscape evolution models's implement Landscape evolution modulation of highly accurate algorithms strongly reduces the shortcomings of rectangular grids while facilitating straightforward processing of in- and output therefore enhancing the ease of modelling.

A Topotoolbox landscape evolution model offers users the flexibility to address a number of issues. It allows users to define different initial conditions such as a flat surface, a randomly disturbed surface or a digital elevation model of a real landscape. Topotoolbox landscape evolution models particularly benefits from the adoption of highly efficient drainage network algorithms that outscore GIS implement Landscape evolution modulations in terms of computational efficiency while maintaining their ability to handle the artefacts (artificial topographic sinks) pertinent in real world digital elevation models (see Table 1 in Schwanghart and Scherler (2014)). Topotoolbox landscape evolution models provide access to different models of hillslope denudation, and allows to model tectonic displacement at any desirable level of detail. Finally, a topotoolbox landscape evolution model provides different numerical schemes to solve the governing equations allowing users to trade-off between computational efficiency and accuracy. To our knowledge, such landscape evolution model versatility is hitherto inexistent and thus adds to the plethora of available Landscape evolution models (Valters, 2016). Its ability to be directly run on available digital elevation models renders topotoolbox landscape evolution models a simulation environment to explore trajectories of landscape evolution under different scenarios of geomorphologic, climatological and tectonic controls.

7. Conclusion

Topotoolbox landscape evolution models v1.0 is a raster based Landscape Evolution Model contained within TopoToolbox. It allows using a flux limiting Total Variation Diminishing Finite Volume Method to solve the stream power law and to simulate lateral displacements. The total variation diminishing-finite volume method solves river incision much more accurate which is reflected in catchment wide erosion rates. Depending on the spatial and temporal resolution used during model runs, first order implicit methods to simulate river incision lead to catchment wide erosion rates which are smeared out over the simulated time span and do not allow to properly capture transient landscapes response. The fact that the impact of numerical schemes is not only altering simulated topography but topotoolbox landscape evolution models 1.0 is embedded within TopoToolbox version 2.2. Topotoolbox landscape evolution models is platform independent and requires MATLAB 2014b or higher and the Image Processing Toolbox. Documentation and user manuals for the most current release version of TopoToolbox and topotoolbox landscape evolution models can be found at the GIT repository in the help folders of the software. The user manual of topotoolbox landscape evolution models includes three tutorials which can be accessed from the command window in MATLAB. To get started: download and extract the main TopoToolbox folder from the repository to a location of your choice.

Reference

- Andrews, D. J. and Bucknam, R. C.: (1987) Fitting degradation of shoreline scarps by a nonlinear diffusion Model, *J. Geophys.Res.*, 92(B12), 12857, doi: 10.1029/JB092iB12p12857,.
- Attal, M., Tucker, G. E., Whittaker, A. C., Cowie, P. a. and Roberts, G. P.: (2008) Modelling fluvial Incision and transient landscape evolution: Influence of dynamic Channel adjustment, *J. Geophys. Res. Earth Surf.*, 515 113(F3), 1–16,doi:10.1029/2007JF000893,.
- Baynes, E. R. C., Attal, M., Niedermann, S., Kirstein, L. a., DuGodunov Method ore, A. J. and Naylor, M.: (2015) Erosion during extreme floodevents dominates Holocene canyon evolution in northeast Iceland, *Proc. Natl. Acad. Sci.*, 112(8), 201415443,doi:10.1073/pnas.1415443112, 2015. 520
- Van der Beek, P. and Braun, J.: (1998) Numerical modelling of landscape evolution on geological time-Scales: a parameter analysis and comparison with the south-eastern highlands of Australia, *Basin Res.*, 10(1), 49–68, doi:10.1046/j.1365-2117.1998.00056.x,.
- Berlin, M. M. and Anderson, R. S.: (2007) Modeling of knickpoint retreat on the Roan Plateau, western Colorado, *J. Geophys. Res.*, 112(F3), F03S06, doi: 10.1029/2006JF000553.
- Bishop, P.: (2007) Long-term landscape evolution: linking tectonics and surface processes, *Earth Surf. Process. Landforms*, 32(3), 329–365, doi: 10.1002/esp,.

- Blöthe, J. H., Korup, O. and Schwanghart, W.: (2015) Large landslides lie low: Excess topography in the Himalaya-Karakoram ranges, *Geology*, 43(6), 523–526, doi:10.1130/G36527.1.
- Braun, J. and Sambridge, M.: (1997) Modelling landscape evolution on geological time scales: A new Method based on irregular 530 spatial discretization, *Basin Res.*, 9(1), 27–52, doi: 10.1046-j.1365-2117.1997.00030.x,
- Braun, J. and Willett, S. D.: (2013) A very efficient O(n), implicit and parallel method to solve the stream Power equation governing fluvial incision and landscape evolution, *Geomorphology*, 180–181, 170–179, doi:10.1016/j.geomorph.2012.10.008.
- Burbank, D. W., Leland, J., Fielding, E., Anderson, R. S., Brozovic, N., Reid, M. R. and Duncan, C.: (1996) Bedrock incision, rock uplift and threshold hillslopes in the northwestern Himalayas, *Nature*, 379(6565), 505–510, doi: 10.1038/379505a0, 1996.535
- Benjamin Campforts, Wolfgang Schwanghart and Gerard Govers (2016) accurate simulation of transient Landscape evolution by eliminating numerical diffusion: the TTLEM 1.0 model *Earth Surf. Dynam. Discuss.*, doi:10.5194/esurf-2016-39, 2016 Manuscript under review for journal *Earth Surf. Dynam.*
- Campforts, B. and Govers, G.: (2015) Keeping the edge: A numerical method that avoids knickpoint Smearing when solving the stream power law, *J. Geophys. Res. Earth Surf.*, 120(7), 1189–1205, doi:10.1002/2014 JF003376, 2015.
- Campforts, B., Vanacker, V., Vanderburgh, J., Baken, S., Smolders, E. and Govers, G.: (2016) Simulating the mobility of meteoric ¹⁰Be in the landscape through a coupled soil-hillslope model (Be2D), *Earth Planet. Sci. Lett.*, 439, 143–157, doi:10.1016/j.epsl.2016.01.017, 540
- Coulthard, T. J., Hancock, G. R. and Lowry, J. B. C.: (2012) Modelling soil erosion with a downscaled Landscape evolution model, *Earth Surf. Process. Landforms*, 37(10), 1046–1055, doi:10.1002/esp.3226.
- Croissant, T. and Braun, J.: (2014) Constraining the stream power law: a novel approach combining a Landscape evolution model and an inversion method, *Earth Surf. Dyn.*, 2(1), 155–166, doi:10.5194/esurf-2-155-2014,
- Crosby, B. T., Whipple, K. X., Gasparini, N. M. and Wobus, C. W.: (2007) Formation of fluvial hanging Valleys: Theory and simulation, *J. Geophys. Res.*, 112(F3), F03S10, doi: 10.1029/2006JF000566.
- Culling, W. E. H.: (1963) Soil Creep and the Development of Hillside Slopes, *J. Geol.*, 71(2), 127–161, doi:10.1086/626891, *Earth Surf. Dynam. Discuss.* doi:10.5194/esurf-2016-39, 2016 Manuscript under review for journal *Earth Surf. Dynam.* Published: 18 July 2016 Author(s) 2016. CC-BY 3.0 License. 17
- DiBiase, R. A. and Whipple, K. X.: (2011) The influence of erosion thresholds and runoff variability on the Relationships among topography, climate, and erosion rate, *J. Geophys. Res. Earth Surf.* 116(F4), F04036, doi: 10.1029/2011JF002095.
- DiBiase, R. A., Whipple, K. X., Heimsath, A. M. and Ouimet, W. B.: (2010) Landscape form and millennial erosion rates in the San Gabriel Mountains, CA, *Earth Planet. Sci. Lett.*, 289(1-2), 134–144, doi:10.1016/j.epsl.2010.09.036.
- Dietrich, W. E., Bellugi, D. G., Sklar, L. S., Stock, J. D., Heimsath, A. M. and Roering, J. J.: (2003) Geomorphic transport laws for predicting landscape form and dynamics, in *Prediction in Geomorphology*, vol. Geophysics, edited by I. Wilcock and I. R., pp. 103–132, American Geophysical Union: Washington, DC.
- Durrant, D. R.: (2010) *Numerical Methods for Fluid Dynamics*, Springer New York, New York, NY., 555
- Fox, M., Goren, L., May, D. A. and Willett, S. D.: (2014) Inversion of fluvial channels for paleo rock uplift rates in Taiwan, *J. Geophys. Res. Earth Surf.*, 119(9), 1853–1875, doi: 10.1002/2014JF003196.
- Gasparini, N. M. and Brandon, M. T.: (2011) A generalized power law approximation for fluvial incision of bedrock channels, *J. Geophys. Res.*, 116(F2), F02020, doi: 10.1029/2009JF001655.
- Gasparini, N. M. and Whipple, K. X.: (2014) Diagnosing climatic and tectonic controls on topography: Eastern flank of the northern 560 Bolivian Andes, *Lithosphere*, (May), 230–250, doi:10.1130/L322.1.
- Gerya, T.: (2010) *Introduction to Numerical Geodynamic Modelling*, Cambridge University Press.
- Glotzbach, C.: (2015) Deriving rock uplift histories from data-driven inversion of river profiles, *Geology*, 43(6), 467–470, doi:10.1130/G36702.1.
- Godunov, S. K.: (1959) A Finite Difference Method for the Computation of Discontinuous Solutions of the

- Equations of Fluid Dynamics, *Math. USSR-Sbornik*, 47(89), 271–306, 1959.
- Goren, L., Willett, S. D., Herman, F. and Braun, J.: (2014) Coupled numerical-analytical approach to Landscape evolution modeling, *Earth Surf. Process. Landforms*, 39(4), 522–545, doi: 10.1002/esp.3514.
- Grimaldi, S., Teles, V. and Bras, R. L.: (2005) Preserving first and second moments of the slope area Relationship during the interpolation of digital elevation models, *Adv. Water Resour.*, 28(6), 583–588, doi: 10.1016/j.advwatres.2004.11.014, 2005.570
- Gulliver, J. S.: (2007) *Introduction to Chemical Transport in the Environment*, Cambridge University Press, Cambridge.
- Harten, A.: (1983) High resolution schemes for hyperbolic conservation laws, *J. Comput. Phys.*, 49(3), 357–393, doi:10.1016/0021-9991(83)90136-5.
- Herman, F. and Braun, J.: (2006) Fluvial response to horizontal shortening and glaciations: A study in the Southern Alps of New Zealand, *J. Geophys. Res.*, 111(F1), F01008, doi:10.1029/2004JF000248, 575
- Hoke, G. D., Isacks, B. L., Jordan, T. E., Blanco, N., Tomlinson, A. J. and Ramezani, J.: (2007) Geomorphic evidence for post-10Ma uplift of the western flank of the central Andes 18°30'–22°S, *Tectonics*, 26(5), doi:10.1029/2006TC002082, 2007.
- Howard, A. D.: (1994) A detachment-limited model of drainage basin evolution, *Water Resour. Res.*, 30(7), 2261–2285, doi: 10.1029/94WR00757.
- Howard, A. D. and Kerby, G.: (1983) Channel changes in badlands. *Geol. Soc. Am. Bull.*, 94(6), 739–752, doi:10.1130/0016-5807(1983)94<739:CCIB>2.0.CO;2.
- Jaruga, A., Arabas, S., Jarecka, D., Pawlowska, H., Smolarkiewicz, P. K. and Waruszewski, M.: (2016) libmpdata++ 1.0: a library Earth Surf. Dynam. Discuss. Doi: 10.5194/esurf-2016-39, 2016 Manuscript under review for journal Earth Surf. Dynam. Published: 18 July 2016c Author(s) 2016. CC-BY 3.0 License. **18** of parallel MPDATA solvers for systems of generalised transport equations, *Geosci. Model Dev.*, 8(4), 1005–1032, doi:10.5194/Godunov Method d-8-1005-2015, 2015.
- Jungers, M. C., Bierman, P. R., Matmon, A., Nichols, K., Larsen, J. and Finkel, R.: (2009) Tracing Hillslope sediment production and transport with in situ and meteoric ¹⁰Be, *J. Geophys. Res.*, 114(F4), 1–16, doi: 10.1029/2008JF001086.
- Kirby, E. and Whipple, K.: (2001) Quantifying differential rock-uplift rates via stream profile analysis, *Geology*, 29(5), 415, doi: 10.1130/0091-7613(2001)029<0415:QDRURV>2.0.CO;2.
- Korup, O.: (2006) Rock-slope failure and the river long profile, *Geology*, 34(1), 45, doi:10.1130/G21959.1.
- Lague, D.: (2014) The stream power river incision model: evidence, theory and beyond, *Earth Surf. Process. Landforms*, 39(1), 38–59, doi:10.1002/esp.3462.
- Lamb, M. P., Mackey, B. H. and Farley, K. A.: (2014) Amphitheater-headed canyons formed by mega flooding at Malad Gorge, Idaho, *Proc. Natl. Acad. Sci. U. S. A.*, 111(1), 57–62, doi:10.1073/pnas.1312251111.
- Larsen, I. J. and Montgomery, D. R.: (2012) Landslide erosion coupled to tectonics and river incision, *Nat. Geosci.*, 5(7), 468–473, doi: 10.1038/ngeo1479, 2012.595
- Lax, P. and Wendroff, B.: (1960) Systems of conservation laws, *Commun. Pure Appl. Math.*, 13(2), 217–237, doi: 10.1002/cpa.3160130205.
- Leer, B.: (1997) Towards the Ultimate Conservative Difference Scheme, *J. Comput. Phys.*, 135(2), 229–248, doi:10.1006/jcph.1997.5704.
- Luke, J. C.: (1972) Mathematical models for landform evolution, *J. Geophys. Res.*, 77(14), 2460–2464, doi: 10.1029/JB077i014p02460.
- Luo, W., Pelletier, J., Duffin, K., Ormand, C., Hung, W., Shernoff, D. J., Zhai, X., Iverson, E., Whalley, K., Gallaher, C. and Furness, W.: (2016) Advantages of Computer Simulation in Enhancing Students' Learning about Landform Evolution: A Case Study Using the Grand Canyon, *J. Geosci. Educ.*, 64(1), 60–73, doi:10.5408/15-080.1,
- Mackey, B. H., Scheingross, J. S., Lamb, M. P. and Farley, K. A.: (2014) Knickpoint formation, rapid propagation, and landscape response following coastal cliff retreat at the last interglacial sea-level high stand: Kaua'i, Hawai'i, *Geol. Soc. Am. Bull.*, 126(7-8), 925–942, doi: 10.1130/B30930.1.
- McGuire, L. A. and Pelletier, J. D.: (2016) Controls on valley spacing in landscapes subject to rapid base-level fall, *Earth Surf. Process. Landforms*, 41(4), 460–472, doi:10.1002/esp.3837.

- Mudd, S. M.: (2016) Detection of transience in eroding landscapes, *Earth Surf. Process. Landforms*, doi: 10.1002/esp.3923,
- Nocedal, J. and Wright, S. J.: (1999) *Numerical Optimization*, Springer, New York.
- Pelletier, J. D.: (2008) *Quantitative Modeling of Earth Surface Processes*, Cambridge University Press, Cambridge.
- Perron, J. T. : (2011) Numerical methods for nonlinear hillslope transport laws, *J. Geophys. Res.*, 116(F2), F02021, doi: 10.1029/2010JF001801, 2011.
- Perron, J. T. and Royden, L.: (2013) An integral approach to bedrock river profile analysis, *Earth Surf. Process. Landforms*, 38(6), 615–630, doi:10.1002/esp.3302, 2013.
- Perron, J. T. and Fagherazzi, S.: (2016) The legacy of initial conditions in landscape evolution, *Earth Surf. Process. Landforms*, *Earth Surf. Dynam. Discuss.* Doi: 10.5194/esurf-2016-39, 2016 Manuscript under review for journal *Earth Surf. Dynam.* Published: 18 July 2016 c Author(s). CC-BY 3.0 License. 1937 (1), 52–63, doi:10.1002/esp.2205, 2011.
- Phillips, J. D., Schwanghart, W. and Heckmann, T.: (2015) Graph theory in the geosciences, *Earth-Science Rev.*, 143, 147–160, doi:10.1016/j.earscirev.2015.02.002,
- Roering, J. J., Kirchner, J. W. and Dietrich, W. E. : (1999) Evidence for nonlinear, diffusive sediment transport on hillslopes and implications for landscape morphology, *Water Resour. Res.*, 35(3), 853–870, doi: 10.1029/1998WR900090, .
- Rosenbloom, N. A. and Anderson, R. S.: (1994) Hillslope and channel evolution in a marine terraced landscape, *J. Geophys. Res.*, 99(94), 13–14, doi: 10.1029/94JB00048,.
- Royden, L. and Perron, J. T.: Solutions of the stream power equation and application to the evolution of river longitudinal profiles, *J. Geophys. Res. Earth Surf.*, 118(2), 497–518, doi:10.1002/jgrf.20031, 2013.
- Schwanghart, W. and Kuhn, N. J.: (2010) TopoToolbox: A set of Matlab functions for topographic analysis, *Environ. Model. Softw.*, 25(6), 770–781, doi:10.1016/j.envsoft.2009.12.002,.
- Schwanghart, W. and Scherler, D.: (2014) Short Communication: TopoToolbox 2 – MATLAB-based software for Topographic analysis and modeling in Earth surface sciences, *Earth Surf. Dyn.*, 2(1), 1–7, doi:10.5194/esurf-2-1-, 2014.630
- Schwanghart, W., Groom, G., Kuhn, N. J. and Heckrath, G.: (2013) Flow network derivation from a high resolution DIGITAL ELEVATION MODEL in a low relief, agrarian landscape, *Earth Surf. Process. Landforms*, 38(13), 1576–1586, doi:10.1002/esp.3452, 2013.
- Seidl, M. and Dietrich, W.: The problem Landscape evolution model of channel erosion into bedrock, *Catena*, 23(Suppl Landscape evolution model), 101–104, 1992.
- Sklar, L. and Dietrich, W. E.: (1998) River longitudinal profiles and bedrock incision models: Stream power and the influence of sediment supply, *Geophys. Monogr. Ser.*, 107, 237–260, doi:10.1029/GODUNOV METHOD 107p0237, 1998.635
- Sklar, L., Dietrich, W. E., Tinkler, J., Wohl, E., Weissel, J. K. and Seidl, M. A.: (1998) *Rivers Over Rock: Fluvial Processes in Bedrock Channels*, edited by J. Tinkler and E. Wohl, American Geophysical Union, Washington, D. C.,.
- Smolarkiewicz, P. K.: (1983) A Simple Positive Definite Advection Scheme with Small Implicit Diffusion, *Mon. Weather Rev.*, 111(3), 479–486, doi: 10.1175/1520-0493(1983)111<0479:ASPDAS>2.0.CO;2, 1983.
- Smolarkiewicz, P. K. and Grabowski, W. W.: (1990) The multidimensional positive definite advection Transport algorithm: 640 nonoscillatory option, *J. Comput. Phys.*, 86(2), 355–375, doi: 10.1016/0021-9991(90)90105-A,.
- Soille, P., Vogt, J. and Colombo, R.: (2003) Carving and adaptive drainage enforcement of grid digital Elevation Models, *Water Resour. Res.*, 39(12), doi:10.1029/2002WR001879,.
- Spiegelman, M. and Katz, R. F.: (2006) A semi-Lagrangian Crank-Nicolson algorithm for the numerical Solution of advection diffusion problem Landscape evolution models, *Geochemistry, Geophys. Geosystems*, 7, 1–12, doi:10.1029/2005GC001073,
- Stock, J. D. and Montgomery, D. R.: (1999) Geologic constraints on bedrock river incision using the Stream power law, *J. Geophys. Res.*, 104(B3), 4983, doi:10.1029/98JB02139, 1999.
- Toro, E. F.: (2009) *Riemann solvers and numerical methods for fluid dynamics-A Practical Introduction*, Springer, New York.
- Tucker, G. E. and Hancock, G. R.: (2010) *Modelling landscape evolution*, *Earth Surf. Process. Landforms*,

- 35(1), 28–50, doi:10.1002/esp.1952.
- Tucker, G. E. and Slingerland, R. L.: (1994) Erosional dynamics, flexural isostasy, and long-lived escarpments: A numerical study, *Earth Surf. Dynam. Discuss.*, doi:10.5194/esurf-2016-39, 2016 Manuscript under review for journal *Earth Surf. Dynam.* Published: 18 July 2016 Author(s) 2016. CC-BY 3.0 License.
- 20 modeling study, *J. Geophys. Res.*, 99(B6), 12229, doi: 10.1029 /94JB00320,.
- Valla, P. G., van der Beek, P. A. and Lague, D.: (2010) Fluvial incision into bedrock: Insights from morphometric analysis and numerical modeling of gorges incising glacial hanging valleys (Western Alps, France), *J. Geophys. Res. Earth Surf.*, 115(F2), doi:10.1029/2009JF001079,.
- Valters, D.: (2016) Modeling Geomorphic Systems: Landscape Evolution, in *Geomorphological Techniques*, vol. 12, edited by S. J. Cook, L. E. Clarke, and J. M. Nield, pp. 1–24, British Society for Geomorphology, London, UK,.
- Vanacker, V., von Blanckenburg, F., Govers, G., Campforts, B., Molina, A. and Kubik, P. W.: (2015) Transient river response, captured by channel steepness and its concavity, *Geomorphology*, 228, 234–243, doi:10.1016 /j.geomorph.2014.09.013, 660.
- Vanmaercke, M., Obreja, F. and Poesen, J.: (2014) Seismic controls on contemporary sediment export in the Siret river catchment, Romania, *Geomorphology*, 216, 247–262, doi:10.1016 /j.geomorph.2014.04.008,.
- Wang, P., Scherler, D., Liu-Zeng, J., Mey, J., Avouac, J.-P., Zhang, Y. and Shi, D.: (2014) Tectonic control of Yarlung Tsangpo Gorge revealed by a buried canyon in Southern Tibet, *Science* (80-), 346(6212), 978–981, doi:10.1126/science.1259041, 665.
- West, N., Kirby, E., Bierman, P., Slingerland, R., Ma, L., Rood, D. and Brantley, S.: (2013) Regolith Production and transport at the Susquehanna Shale Hills Critical Zone Observatory, Part 2: Insights from meteoric ¹⁰Be, *J. Geophys. Res. Earth Surf.*, 118(3), 1877–1896, doi:10.1002/jgrf.20121,.
- Whipple, K. X. and Meade, B. J.: (2004) Controls on the strength of coupling among climate, erosion, and Deformation in two-sided, frictional orogenic wedges at steady state, *J. Geophys. Res. Earth Surf.*, 109(F1), n/a–n/a, doi:10.1029 /2003JF000019,.
- Whipple, K. X. and Tucker, G. E.: (1999) Dynamics of the stream-power river incision model: Implications for height limits of mountain ranges, landscape response timescales, and research needs, *J. Geophys. Res.*, 104(B8), 17661, doi:10.1029/1999JB900120, 675
- Whittaker, A. C., Cowie, P. A., Attal, M., Tucker, G. E. and Roberts, G. P.: (2007) Contrasting transient and steady-state rivers crossing active normal faults: New field observations from the central Apennines, Italy, *Basin Res.*, 19(4), 529–556, doi:10.1111/j.1365-2117.2007.00337.x,.
- Willett, S. D.: (1999) Orogeny and orography: The effects of erosion on the structure of mountain belts, *J. Geophys. Res. Solid Earth*, 104(B12), 28957–28981, doi:10.1029/1999JB900248, 680
- Willett, S. D., Slingerland, R. and Hovius, N.: (2001) Uplift, Shortening, and Steady State Topography in Active Mountain Belts, *Am. J. Sci.*, 301(April/May), 455–485, doi:10.2475/ajs.301.4-5.455,.
- Willett, S. D., McCoy, S. W., Perron, J. T., Goren, L. and Chen, C.-Y.: (2014) Dynamic reorganization of River Basins. *Science*, 343(6175), 1248765, doi:10.1126/science.1248765,.
- Willgoose, G., Bras, R. L. and Rodriguez-Iturbe, I.: (1991a) A coupled channel network growth and Hillslope Evolution model: 1. 685 Theory, *Water Resour. Res.*, 27(7), 1671–1684, doi: 10.1029 /91WR00935, 1991a.
- Willgoose, G., Bras, R. L. and Rodriguez-Iturbe, I.: (1991b) Results from a new model of river basin Evolution, *Earth Surf. Process. Landforms*, 16(3), 237–254, d
-